

University of Windsor

## Scholarship at UWindor

---

Electronic Theses and Dissertations

Theses, Dissertations, and Major Papers

---

2022

# Application of Artificial Neural Networks to Predict Local Bridge Pier Scour

Mia Marrocco  
*University of Windsor*

Follow this and additional works at: <https://scholar.uwindsor.ca/etd>



Part of the [Civil Engineering Commons](#)

---

### Recommended Citation

Marrocco, Mia, "Application of Artificial Neural Networks to Predict Local Bridge Pier Scour" (2022).  
*Electronic Theses and Dissertations*. 8933.  
<https://scholar.uwindsor.ca/etd/8933>

This online database contains the full-text of PhD dissertations and Masters' theses of University of Windsor students from 1954 forward. These documents are made available for personal study and research purposes only, in accordance with the Canadian Copyright Act and the Creative Commons license—CC BY-NC-ND (Attribution, Non-Commercial, No Derivative Works). Under this license, works must always be attributed to the copyright holder (original author), cannot be used for any commercial purposes, and may not be altered. Any other use would require the permission of the copyright holder. Students may inquire about withdrawing their dissertation and/or thesis from this database. For additional inquiries, please contact the repository administrator via email ([scholarship@uwindsor.ca](mailto:scholarship@uwindsor.ca)) or by telephone at 519-253-3000ext. 3208.

# **Application of Artificial Neural Networks to Predict Local Bridge Pier Scour**

By

**Mia Marrocco**

A Thesis

Submitted to the Faculty of Graduate Studies  
through the Department of Civil and Environmental Engineering  
in Partial Fulfillment of the Requirements for  
the Degree of Master of Applied Science  
at the University of Windsor

Windsor, Ontario, Canada

2022

© 2022 Mia Marrocco

# Application of Artificial Neural Networks to Predict Local Bridge Pier Scour

by

**Mia Marrocco**

APPROVED BY:

---

P. Williams  
IIHR – Hydrosience & Engineering (University of Iowa)

---

M. Belalia  
Department of Mathematics and Statistics

---

T. Bolisetti  
Department of Civil and Environmental Engineering

---

R. Balachandar, Co-Advisor  
Department of Civil and Environmental Engineering

---

R. Barron, Co-Advisor  
Department of Mechanical, Automotive, and Materials Engineering

December 7, 2022

## DECLARATION OF ORIGINALITY

I hereby certify that I am the sole author of this thesis and that no part of this thesis has been published or submitted for publication.

I certify that, to the best of my knowledge, my thesis does not infringe upon anyone's copyright nor violate any proprietary rights and that any ideas, techniques, quotations, or any other material from the work of other people included in my thesis, published or otherwise, are fully acknowledged in accordance with the standard referencing practices. Furthermore, to the extent that I have included copyrighted material that surpasses the bounds of fair dealing within the meaning of the Canada Copyright Act, I certify that I have obtained a written permission from the copyright owner(s) to include such material(s) in my thesis and have included copies of such copyright clearances to my appendix.

I declare that this is a true copy of my thesis, including any final revisions, as approved by my thesis committee and the Graduate Studies office, and that this thesis has not been submitted for a higher degree to any other University or Institution.

## ABSTRACT

Accurate equilibrium scour depth and width estimations are essential to both safe and economic designs of bridge foundations. Review of current scour estimation methods demonstrate that the empirical equations produce scour values that are overestimated, resulting in uneconomical designs. In the current investigation, artificial neural networks (ANNs) were optimized and applied to scour data under laboratory conditions, field conditions, and a combination of the two conditions. Additionally, physics-based parameters – in place of empirical parameters (e.g., shape factors) – and parameters incorporating blockage effects were introduced as input parameters to the ANNs in an attempt to improve scour predictions. Finally, ANNs were applied to scour width estimations to investigate the applicability of machine learning tools to scour width prediction. For each of the ANNs developed, a sensitivity analysis was conducted to ensure each of the input parameters selected had significant value on the prediction models. Sensitivity analyses also allow for a further understanding of each of the parameters' influence on the models.

## DEDICATION

To Lola

## ACKNOWLEDGEMENTS

I would like to express my deepest gratitude to Dr. Ram Balachandar and Dr. Ronald Barron for their continuous guidance, support, and patience over the last two years. I would also like to thank the members of my committee, Dr. Mohamed Belalia, Dr. Tirupati Bolisetti, and Dr. Priscilla Williams for their time and suggestions.

Thank you to Emanuel Raad, Dr. Akindolu Dada, Dr. Vesselina Roussinova, Mohamed Kharbeche, John McGurn, and the rest of the research group for their insight and support. Thank you to the NSERC organization, for their financial contributions to my work through the Canada Graduate Scholarship program.

To Lucas Dodson, Anna Simone, and Liz Sweeny, thank you for your continuous encouragement and friendship over the years.

To my mom and dad, thank you for everything you have done for me to help me get to where I am today, and your endless love and support through it all. Thank you to my siblings, Melise, Matteo, and Massimo for putting up with me during the lockdown (and life in general).

Finally, I would like to thank Scott Dos Santos, for always believing in me and for your constant patience, love, and support.

## TABLE OF CONTENTS

DECLARATION OF ORIGINALITY .....	iii
ABSTRACT .....	iv
DEDICATION .....	v
ACKNOWLEDGEMENTS .....	vi
LIST OF TABLES .....	ix
LIST OF FIGURES .....	xi
LIST OF APPENDICES .....	xiv
LIST OF ABBREVIATIONS/SYMBOLS .....	xv
CHAPTER 1 .....	1
1.1 Introduction .....	1
1.2 Objectives .....	4
1.3 Scope of Work .....	5
1.4 Organization of Thesis .....	5
CHAPTER 2 .....	6
2.1 The Scour Process .....	6
2.2 Parameters Affecting Scour .....	7
2.2.1 Blockage Effects .....	9
2.2.2 Pier Length .....	10
2.2.3 Pier Shape .....	11
2.2.4 Flow Separation Velocity from Pier .....	13
2.3 Scour Estimation Methods .....	13
2.3.1 Scour Depth Estimation .....	14
2.3.2 Scour Width Estimation .....	17
2.4 Artificial Neural Networks (ANN) .....	19
2.4.1 ANNs and Scour Predictions .....	21
CHAPTER 3 .....	26
3.1 Overview .....	26
3.2 Laboratory Data .....	26
3.2.1 Data Collection .....	26
3.2.2 Resulting Database .....	28
3.2.3 Scour Width Data .....	30
3.3 Field Data .....	30
3.3.1 Data Collection .....	30
3.3.2 Final Database .....	32

3.4 Combined Dataset.....	34
3.4.1 Final Database.....	34
CHAPTER 4 .....	37
4.1 Model Development.....	37
4.1.1 Optimization of Hyperparameters.....	38
4.1.2 Sensitivity Analysis .....	40
4.2 Model Evaluation.....	40
CHAPTER 5 .....	42
5.1 Laboratory-trained Model.....	42
5.1.1 Inclusion of Blockage Effects.....	43
5.1.2 Sensitivity Analysis .....	45
5.1.3 Comparison to Prediction Equations .....	46
5.1.4 Field Estimations .....	47
5.2 Field Model.....	48
5.2.1 Shape Factors.....	50
5.2.2 Inclusion of Flow Separation Velocity .....	51
5.2.3 Sensitivity Analysis .....	52
5.2.4 Comparison to Equations.....	53
5.3 Combined Model .....	55
5.3.1 Shape Factors.....	56
5.3.2 Inclusion of Flow Separation Velocity .....	57
5.3.3 Sensitivity Analysis .....	58
5.3.4 Comparison to Other Prediction Models .....	59
5.4 Scour Width Model.....	63
5.4.1 Inclusion of Blockage Effects.....	64
5.4.2 Sensitivity Analysis .....	66
5.4.3 Comparison to Prediction Equation.....	67
CHAPTER 6 .....	71
6.1 Summary .....	71
6.2 Recommendations.....	73
REFERENCES .....	74
APPENDICES .....	80
Appendix A: Software Acknowledgements.....	80
Appendix B: Additional Results .....	81
VITA AUCTORIS .....	87

## LIST OF TABLES

Table 1.1: Bridge failures due to scour .....	2
Table 2.1: Shape factors proposed for various pier shapes.....	12
Table 2.2: Input parameters utilized in literature for development of ANNs.....	25
Table 3.1: Laboratory data resources .....	27
Table 3.2: Statistical parameters for non-dimensional laboratory data .....	29
Table 3.3: Statistical parameters for non-dimensional laboratory scour width data.....	30
Table 3.4: Statistical parameters for non-dimensional field data .....	34
Table 3.5: Statistical parameters for non-dimensional combination data.....	36
Table 4.1: Hyperparameters optimized using Optuna framework.....	39
Table 4.2: Example input parameters used to conduct sensitivity analysis .....	40
Table 5.1: Results from laboratory-trained ANNs including and excluding blockage effects .....	44
Table 5.2: Sensitivity analysis results for laboratory-trained ANN.....	46
Table 5.3: Comparison of laboratory ANN to empirical formulae.....	46
Table 5.4: Results from applying different shape factors to the field-trained ANN.....	51
Table 5.5: Comparison of field-trained ANNs with varying velocity scales.....	52
Table 5.6: Sensitivity analysis results for field-trained ANN.....	53
Table 5.7: Comparison of error values from field ANN against empirical formulae.....	55
Table 5.8: Results of applying various shape factors to combined-trained model .....	57
Table 5.9: Comparison of combined ANNs with varying velocity scales.....	57
Table 5.10: Sensitivity analysis results for combined-trained ANN .....	59
Table 5.11: Comparison of error values from combined ANN against empirical formulae .....	62
Table 5.12: Comparison of present ANN to others found in literature .....	62

Table 5.13: Results of blockage effects investigation on scour width model.....	65
Table 5.14: Comparison of scour width ANNs with varying velocity scales.....	65
Table 5.15: Sensitivity analysis results for scour width ANN.....	67
Table 5.16: Comparison of error values from scour width model to HEC-18 (2001) scour width equation.....	68
Table 5.17: Comparison of error values from scour width model to various empirical $d_{sc}/D$ equations .....	70
Table 6.1: Summary of ANNs developed.....	72

## LIST OF FIGURES

Figure 2.1: Schematic of local scour around a bridge pier .....	9
Figure 2.2: Scour hole and deposition centerline profiles for constant $D/d_{50}$ (extracted from D’Alessandro, 2013).....	10
Figure 2.3: Variation of equilibrium scour depth with pier aspect ratio and pier shape (extracted from Kharbeche, 2022) .....	11
Figure 2.4: Predicted versus measured scour width values .....	18
Figure 2.5: General schematic of an artificial neural network.....	19
Figure 2.6: Division of data sets in Toth and Brandimarte (2011) investigation .....	23
Figure 3.1: Pair-wise plots for non-dimensional laboratory data .....	29
Figure 3.2: Variation of k parameter with blockage ratio and pier shape (extracted from Williams et al., 2019) .....	32
Figure 3.3: Pair-wise plots for non-dimensional field data.....	33
Figure 3.4: Pair-wise plots for non-dimensional combination data.....	35
Figure 5.1: Predicted vs. observed $d_{sc}/D$ for laboratory-trained model .....	43
Figure 5.2: Predicted vs. measured $d_{sc}/D$ for laboratory ANN (a) excluding $D/B$ and (b) re-optimized without $D/B$ .....	45
Figure 5.3: Predicted versus observed $d_{sc}/D$ for the (a) Froelich (1988) equation, (b) HEC-18 equation, (c) S/M (2011) equation, and (d) Williams (2016) equation applied to laboratory data .....	47
Figure 5.4: Predicted vs. measured $d_{sc}/D$ for field scour estimations produced from the laboratory-trained ANN .....	48
Figure 5.5: Predicted vs. actual $d_{sc}/D$ for field-trained ANN .....	49

Figure 5.6: Predicted vs. observed $d_{se}/D$ for field-trained ANN with $C_D$ .....	51
Figure 5.7: Predicted versus observed $d_{se}/D$ for the (a) Froelich (1988) equation, (b) HEC-18 equation, (c) S/M (2011) equation, and (d) Williams (2016) equation applied to field data.....	54
Figure 5.8: Predicted vs. measured $d_{se}/D$ for combination ANN .....	56
Figure 5.9: Predicted vs. actual $d_{se}/D$ for combination ANN with $U_s/U_c$ .....	58
Figure 5.10: Predicted versus observed $d_{se}/D$ for the (a) Froelich (1988) equation, (b) HEC-18 equation, (c) S/M (2011) equation, and (d) Williams (2016) equation applied to combination data .....	61
Figure 5.11: Predicted vs. measured $d_{se}/D$ and $w_s/D$ for scour width model.....	64
Figure 5.12: Predicted vs. actual $d_{se}/D$ and $w_s/D$ for scour width ANN with $U_s/U_c$ .....	66
Figure 5.13: Predicted vs. observed $w_s/D$ for HEC-18 (2001) scour width equation, with $d_{se}/D$ values known and unknown.....	69
Figure 5.14: Predicted versus observed $d_{se}/D$ for the (a) Froelich (1988) equation, (b) HEC-18 equation, (c) S/M (2011) equation, and (d) Williams (2016) equation applied to depth data within scour width database .....	70
Figure B.1: Predicted vs. observed $d_{se}/D$ for field ANN with Neill shape factor.....	81
Figure B.2: Predicted vs. observed $d_{se}/D$ for field ANN with A&O shape factor .....	81
Figure B.3: Predicted vs. observed $d_{se}/D$ for field ANN with $k$ .....	82
Figure B.4: Predicted vs. observed $d_{se}/D$ for field ANN with $U_s/U_c$ .....	82
Figure B.5: Predicted vs. observed $d_{se}/D$ for combination ANN with HEC-18 shape factor.....	83
Figure B.6: Predicted vs. observed $d_{se}/D$ for combination ANN with Neill shape factor .....	83
Figure B.7: Predicted vs. observed $d_{se}/D$ for combination ANN with A&O shape factor .....	84
Figure B.8: Predicted vs. observed $d_{se}/D$ for combination ANN with $k$ .....	84

Figure B.9: Predicted vs. observed  $d_{se}/D$  and  $w_s/D$  for scour width ANN re-optimized without  $D/B$  ..... 85

Figure B.10: Predicted vs. observed  $d_{se}/D$  and  $w_s/D$  for scour width ANN with  $k$  ..... 85

Figure B.11: Predicted vs. observed  $d_{se}/D$  and  $w_s/D$  for scour width ANN with  $F_{ds}$  ..... 86

## LIST OF APPENDICES

Appendix A: Software Acknowledgements .....	80
Appendix B: Additional Results .....	81

## LIST OF ABBREVIATIONS/SYMBOLS

ANN	artificial neural network
ANFIS	adaptive neuro-frenzy inference system
B	channel width
$C_D$	drag coefficient
CSU	Colorado State University
D	pier diameter or width
D/B	blockage ratio
D/d <sub>50</sub>	relative coarseness
d <sub>50</sub>	median sediment size/diameter
DNN	deep neural network
D <sub>p</sub>	projected width of pier
d <sub>se</sub>	equilibrium scour depth
d <sub>se</sub> /D	relative equilibrium scour depth
F <sub>ds</sub>	densimetric Froude number based on separation velocity
Fr	Froude number
g	gravitational acceleration
h	flow depth
h/D	flow shallowness
HEC-18	Hydraulic Engineering Circular No. 18
k	ratio of flow separation velocity to approach flow velocity
K <sub>2</sub>	correction factor for angle of attack of flow (HEC-18)
K <sub>3</sub>	correction factor for bed condition (HEC-18)
K <sub>4</sub>	correction factor for armoring condition (HEC-18)
k <sub>b</sub>	bed sediment shape factor
K <sub>s</sub>	pier shape factor (HEC-18)
K <sub>SF</sub>	pier shape factor (Froehlich)
K <sub>ws</sub>	bottom width of scour hole related to depth of scour
L	pier length
L/D	pier aspect ratio

MAE	mean absolute error
MAPE	mean absolute percent error
MSE	mean squared error
n	number of data points
$N_s$	shape factor (Neill)
R	coefficient of correlation
RBF	radial-bias function
ReLU	rectified linear unit
S/M	Sheppard-Melville
SG	specific gravity of bed material
U	mean flow velocity
$u^*_c$	critical shear velocity of bed material
$U/U_c$	flow intensity
$U_c$	critical velocity of bed material
$U_s$	flow separation velocity from bridge pier
USGS	United States Geological Survey
$w_s$	width of scour hole
$w_s/D$	relative scour width
x	ANN input parameter
$X_{iN}$	scaled input value
$X_{max}$	maximum of input values
$X_{min}$	minimum of input values
$y_i$	observed value
$\hat{y}_i$	predicted value
$\alpha$	pier shape
$\beta$	pier orientation
$\theta$	flow angle of incidence
$\mu$	dynamic viscosity of fluid
$\rho$	fluid density
$\rho_s$	bed sediment density
$\sigma_g$	uniformity of sediment particle size distribution

$\sigma_N$	standard deviation of scaled input values
$\sigma_x$	standard deviation of input values
$\tau$	near-bed shear stress
$\varphi$	bed sediment angle of repose
$\bar{X}$	mean of input values
$\bar{y}$	mean of observed values
$\bar{\hat{y}}$	mean of predicted values
$\overline{X_N}$	mean of scaled input values

# CHAPTER 1

## INTRODUCTION

### **1.1 Introduction**

It is important that engineering infrastructure, such as bridges, are monitored and investigated as they reach the end of service life and/or potential failure. Understanding the main causes of bridge failure is also imperative to the design of new structures to ensure that these issues be mitigated in future designs. Aside from safety concerns that arise from bridge failure, there are various other implications to consider. The failure, and subsequent reconstruction, of bridge structures can have negative economic, environmental, and societal impacts. Through multiple investigations, it has been established that scour and scour-related complications are the leading cause of bridge failure in North America, as well as other areas of the world, with over 50% percent of bridge failures being attributed to scour and scour-related complications. Table 1.1 summarizes results from five separate investigations of bridge failures, where cases of bridge failure and their causes were investigated (Cook, 2014; Garg et al., 2022; Miroff, 2007; Shirole & Holt, 1991; Wardhana & Hadipriono, 2003).

Scouring around of bridge piers is an ongoing concern, with a Canadian bridge collapsing as recently as November 2021, after a flood event caused extensive damage of the bridge foundation. The bridge was located along British Columbia's Coquihalla Highway at Juliet Creek. The flood caused many other infrastructure issues along the highway, causing the highway to be completely shut down. This caused many residents, truck drivers and others to take alternate routes, increasing travel time by as much as four hours and fuel costs. Residents

and travelers in some near-by towns were even stranded and cut-off from the rest of the province (Braich & Mendoza, 2022).

*Table 1.1: Bridge failures due to scour*

<b>Resource</b>	<b>Year</b>	<b>Location</b>	<b>Bridges surveyed</b>	<b>Failures caused by scour</b>
Shirhole and Holt	1991	North America	823	60% (scour and scour-related complications)
Wardhana and Hadipriono	2003	North America	500+	53% (flood and scour)
Briaud (as quoted by Miroff)	2007	North America	1502	60% (scour around foundation)
Cook	2014	North America	691	55% (scour and scour-related complications)
Garg, Chandra and Kumar	2022	India	2010	51% (flood and scour)

Scour refers to the erosion or removal of bed material in a natural flow system due to the acceleration of flowing water. Scour is generally categorized into two types: general and localized scour. General scour is the movement of sediment due to environmental or seasonal changes to the velocity of flow (i.e. regardless of the presence of infrastructure or change in channel geometry). Localized scour occurs when an obstruction to the flow – bridge piers, abutments, etc. – causes an increase in flow velocity and erosion of sediment and can be further divided into contraction and local scour. Contraction scour is caused when there is a contraction of the channel, whether from a natural narrowing or from a bridge. The current research focusses on local scour which is the removal of bed material directly induced by the presence of a bridge pier.

Currently, bridge foundation design is based on approved code-specified methods with respect to bridge pier scour. These methods are typically empirical equations developed by curve-fitting to experimental data, obtained from laboratory experiments. There have been many

cautions proposed for the estimation of equilibrium scour depth, especially when extrapolating to field situations. Recent research shows that there are several deficiencies with current prediction equations, including unnecessarily high estimates (Williams et al., 2013). These high scour depth estimations could lead to over-engineered and uneconomical foundation designs. Such designs would require excessive materials and add to the construction cost. Many challenges arise in developing an accurate equation with curve-fitting methods with laboratory data. These challenges include the complexity of the scour mechanism, the inability to quantify all scour influences, and the limitations of geometric and flow conditions. One method of mitigating these challenges is the use of artificial neural networks (ANN) – mathematical machine-learning models that are derived from an analogy to brain cells and biological networks. Additionally, scale effects of hydraulic modelling create difficulty in obtaining relevant experimental data to investigate real-world situations; experimental results do not necessarily carry over to field observations. The ability to develop an accurate scour prediction model based on field measurements, such as with an ANN, would help this issue.

When developing machine learning models, it is valuable to include input parameters that have physical meaning. Although the underlying physics of the problem does not need to be known when developing a neural network, the addition of physics-based parameters aids the network in learning the training data provided. The inclusion of physics-based parameters would allow the model to train more accurately and efficiently, reducing the computational requirements while producing more favourable results.

Recent research at the University of Windsor, conducted by Williams (2016) included developing a new scour estimation model which accounts for the densimetric Froude number and blockage effects, as it was discovered that both these parameters have a significant effect on the

scour depth. Additional research was carried out by Kharbeche (2022) to expand this research to also include pier shape and aspect ratio ( $L/D$ ) effects. However, the scour estimation methods that were proposed by these researchers were created by fitting empirical equations to data obtained from laboratory experiments. These new estimation methods were also not evaluated for real-world use in field applications. It is important that the scour depth prediction models be accurate for field use, as those are the values utilized in bridge foundation design. There is also a need to analyse the parameters used to develop a scour prediction model, to ensure that the parameters being used in the methods are producing the most accurate results possible.

In addition to scour depth estimation methods, scour width estimation methods are also essential to bridge foundation design, especially in the design of scour countermeasures, such as the use of riprap. Knowledge of scour width also aids in other aspects of bridge foundation design – i.e., when there are more than one bridge piers in proximity to one another, it is important to determine if the scour holes will overlap with each other. Hence, there is also a need for accurate scour width estimations.

## **1.2 Objectives**

This research will further investigate the feasibility of creating scour prediction methods based on field-obtained data, and not entirely relying on lab-run experiments. The efficacy of current parameters utilized, as well as new ones, on bridge pier scour prediction will be evaluated. The objectives of this thesis include:

- To evaluate current parameters used in pier scour prediction models and investigate application of physics-based inputs.

- Improve scour predictions to be used in practice through utilizing a combination of laboratory and field data.
- Investigate applicability of neural networks on scour width predictions.

### **1.3 Scope of Work**

The current research consists of analysing data to improve scour depth and width estimation methods. Multiple artificial neural networks were developed using PyTorch Lightning in Google's Collaboratory workspace. Of the networks developed, two models were selected as final scour prediction models. The scope of work for this research did not involve investigation of the physics of flow around bridge piers.

### **1.4 Organization of Thesis**

The thesis is divided into five chapters. Chapter 2 contains a literature review of the scour process, current prediction methods, and artificial neural networks. An outline of the methodology used for scour data collection and analysis is presented in Chapter 3. Neural networks are introduced in Chapter 4, followed by a discussion of the scour prediction model development and evaluation. The fifth chapter presents the results and analysis of the research. Finally, Chapter 6 includes the conclusions, recommendations and discussion of future work.

## CHAPTER 2

### LITERATURE REVIEW

#### 2.1 The Scour Process

Scour is defined as the movement or erosion of channel bed sediment due to flowing water and can be divided into three types – general, contraction, and local scour. The current research focusses on local scour around bridge piers, which can be defined as the erosion of bed material induced by the change of flow due to the presence of a bridge pier. Local scour may also occur around other structures, common examples include abutments, sluice gates and spillways. The scouring mechanism around a bridge pier is complex. The flow field consists of a horseshoe vortex around the pier, downflow on the upstream surface of the pier, trailing vortices, wake vortices, or any combination of these. Initiation of the scour process occurs at the pier sides when the flow acceleration around the sides of the pier results in a pressure decrease around the pier in the downstream direction. A ring of scoured material is then created along the sides of the pier as the scour increases in the upstream direction, until the upstream face of the pier is reached (Guo, 2012). The downward flow velocity increases, caused by the downward pressure gradient that is created at the pier face. This increase in downward flow velocity induces the scouring action. The horseshoe vortex is created when this downflow curls up and around itself, getting trapped in the scour ring and causing a rapid removal of sediment (Guo, 2012). The bed material continues to erode until an equilibrium scour depth ( $d_{se}$ ) is reached.

The state of equilibrium scour varies with the conditions of the scouring taking place. The conditions can be either clear-water – when the bed material is at rest – or live-bed – when bed material is being transported by the approach flow. In clear-water conditions, the equilibrium

state is reached at the point in time when bed material is no longer being removed from the scour hole, as the velocity of the circulating flow in the hole is no longer capable of doing so (Chiew, 1984). This occurs when the critical shear stress of the bed material at the bottom of the scour hole is equal to the shear stress caused by the horseshoe vortex (Deng & Cai, 2010). For live-bed conditions, the equilibrium condition can be defined as the scour depth at which the rate of sediment transport out of the scour hole is equal to the rate of sediment transport into the hole (Chiew, 1984).

The equilibrium scour depth around a bridge pier is an important parameter in the design of bridge foundations. Accurate scour depth estimates are essential to not only safe, but economic bridge pier designs. An underestimation of equilibrium scour depth will result in the bridge pier placed at an insufficient depth, in which case the pier may be undermined from scour, causing the bridge to fail. If the equilibrium scour depth is overestimated, the bridge foundation may be over-engineered, resulting in an uneconomical design of the bridge piers. In addition to scour depth estimations, accurate scour width estimations are also significant, especially with the design of scour countermeasures and situations where piers are in proximity to one another or to an abutment. Knowledge of the width of the scour hole aids in the determination of the extent of scour countermeasure (e.g. riprap) required. It is also critical to ensure that the local scour holes do not overlap with one another. Furthermore, accurate estimations of scour width are essential from a waterway standpoint, as the high turbulence in these regions affects water vehicles (Pandey et al., 2017).

## **2.2 Parameters Affecting Scour**

The equilibrium scour depth around a bridge pier is influenced by many different parameters. A majority of these parameters can be categorized into three general groups: flow properties, bed

sediment characteristics, and pier geometry (Melville & Chiew, 1999). The flow properties may be further divided into fluid specific and flow specific parameters. Since scour is a temporal process, time is another parameter that should be considered, however, it does not fit into the three aforementioned categories. The following is a breakdown of the parameters affecting equilibrium scour depth:

- Flow properties:
  - Fluid: density ( $\rho$ ), dynamic viscosity ( $\mu$ ), temperature
  - Flow: flow depth ( $h$ ), energy slope, near-bed shear stress ( $\tau$ ), angle of incidence ( $\theta$ ), mean flow velocity ( $U$ )
- Bed sediment characteristics: sediment density ( $\rho_s$ ), median sediment size/diameter ( $d_{50}$ ), uniformity of particle size distribution ( $\sigma_g$ ), cohesiveness, shape factor ( $k_b$ ), angle of repose ( $\phi$ ), fall velocity, and critical velocity of the bed material ( $U_c$ ).
- Pier geometry: pier diameter or transverse width ( $D$ ), length ( $L$ ), shape ( $\alpha$ ), surface condition, pier orientation ( $\beta$ ), and debris accumulation.

A schematic of local scour around a bridge pier is shown in Figure 2.1.

Typically, the above list of parameters is reduced to those which have the greatest influence on  $d_{se}$  for analysis. Research has shown that

$$d_{se} = f(\rho, \mu, U, U_c, h, \rho_s, d_{50}, \sigma_g, g, D, L, \alpha, \beta) \quad (2.1)$$

where  $g$  is the gravitational acceleration. The number of parameters may be further reduced through dimensional analysis. Typically, the equilibrium scour depth is normalized by either the

flow depth or pier diameter. Using the pier diameter, the dimensionless form of the equation for equilibrium scour depth is presented as:

$$\frac{d_{se}}{D} = f\left(\frac{U}{U_c}, \frac{U}{\sqrt{gh}}, \frac{h}{D}, \frac{D}{d_{50}}, \frac{\rho U D}{\mu}, \frac{L}{D}, \alpha\right). \quad (2.2)$$

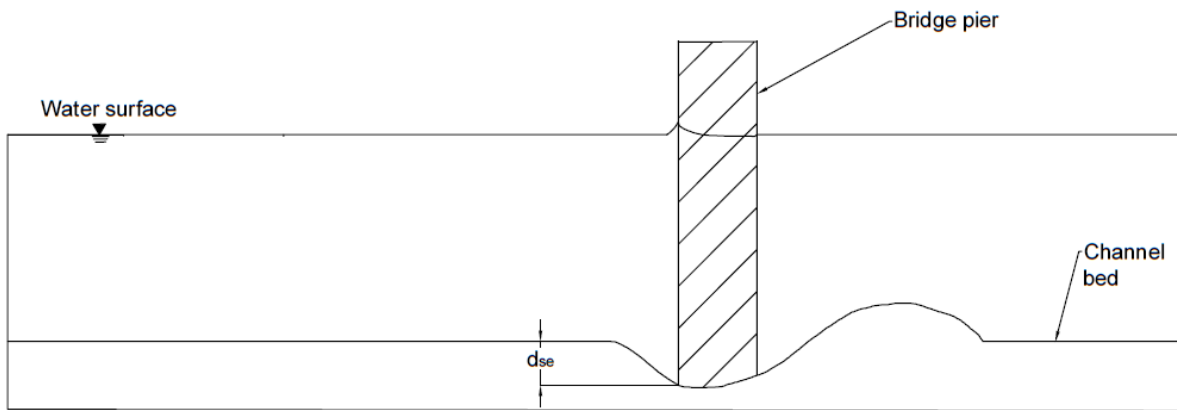


*Figure 2.1: Schematic of local scour around a bridge pier*

### **2.2.1 Blockage Effects**

Channel blockage is often not considered as a governing parameter affecting equilibrium scour depth as it has been suggested that blockage effects are negligible when the blockage ratio is less than 10% (Chiew, 1984), where blockage ratio is defined as the pier diameter ( $D$ ) divided by the channel width ( $B$ ). However, recent research has shown that changes in scour geometry were observed with small changes in blockage ratio for  $D/B$  less than 10% (D'Alessandro, 2013; Hodi, 2009; Tejada, 2014). Hodi (2009) compared scouring around bridge piers for varying blockage ratios; blockage effects were detected when the blockage ratio ( $D/B$ ) was in the range of  $2.2\% < D/B < 5\%$ . D'Alessandro (2013) investigated the effect of blockage ratio on local scour while maintaining identical flow conditions (i.e., blockage ratio was varied between tests while all other flow conditions remained the same). It was discovered that both equilibrium scour depth and scour width are affected by blockage ratio. Differences in scour geometry were

observed for small changes in blockage ratio, as demonstrated in Figure 2.2. Tejada (2014) conducted clear-water scour experiments with various cohesive materials and found that blockage ratio has “minimal” influence on local scour depth when the relative coarseness ( $D/d_{50}$ ) is less than 100.

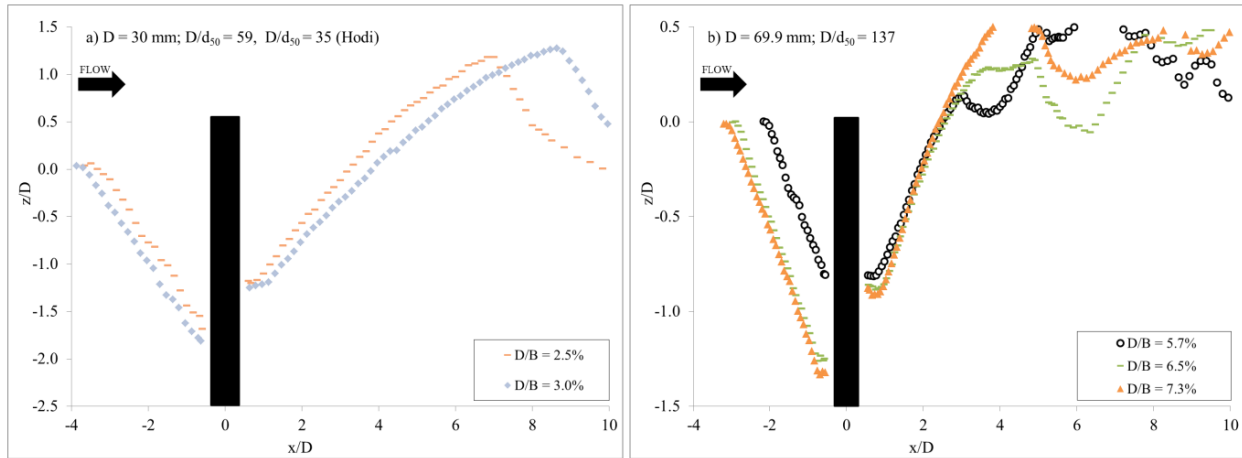


Figure 2.2: Scour hole and deposition centerline profiles for constant  $D/d_{50}$  (extracted from D’Alessandro, 2013)

## 2.2.2 Pier Length

In many scour prediction models, the length of the pier, or pier aspect ratio ( $L/D$ ), is not considered when the incoming flow is inline with the pier (i.e. angle of attack of the approach flow is  $0^\circ$ ). When developing a scour depth prediction model, Toth & Brandimarte (2011) stated “the pier length has no influence on the upstream scour when the attack angle is zero.” The HEC-18 equation (Richardson & Davis, 2001) – which is used by a majority of jurisdictions in the United States – also follows this logic, as the pier aspect ratio is only considered within the correction factor for angle of attack of flow ( $K_2$ ). The equation to calculate the  $K_2$  correction factor is

$$K_2 = \left( \cos \theta + \frac{L}{D} \sin \theta \right)^{0.65} \quad (2.3)$$

where it can be seen that the pier aspect ratio has no influence when the angle of attack is equal

to zero. Recent research at the University of Windsor investigated the role of aspect ratio on local scour (Kharbeche, 2022). Through this investigation, it was discovered that, for similar pier shapes, as the  $L/D$  ratio increased, the equilibrium scour depth decreased when the approach flow angle of attack was equal to zero. This is demonstrated in Figure 2.3, where the variation of equilibrium scour depth is plotted against pier aspect ratio for different pier shapes. The current research will include the pier aspect ratio in scour prediction models based on the results of the investigation conducted by Kharbeche (2022). Further analysis will be conducted to obtain a better understanding of the influence of the pier aspect ratio in the scour prediction model(s) developed and whether the parameter adds value to the scour estimates.

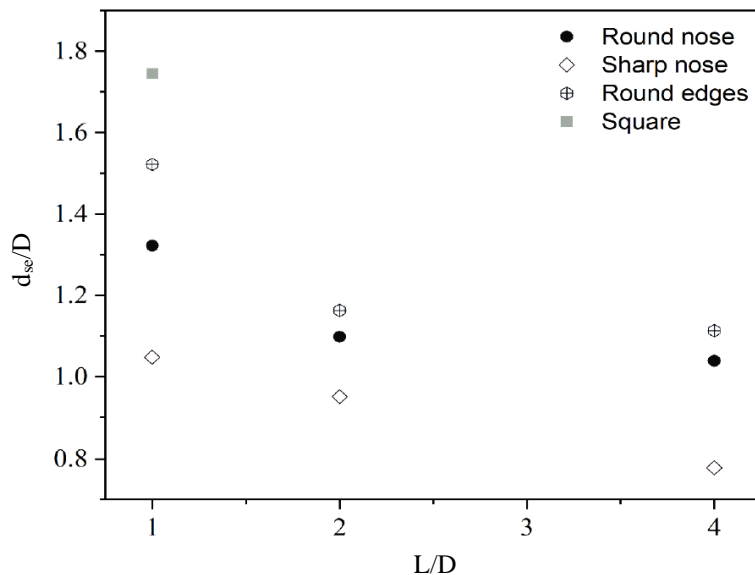


Figure 2.3: Variation of equilibrium scour depth with pier aspect ratio and pier shape (extracted from Kharbeche, 2022)

### 2.2.3 Pier Shape

In practice, there are many different pier shapes that may be used in bridge design. There have been various investigations, both experimental and computational, on the effect of pier shape on scour depth (Al-Shukur and Obeid, 2016; Breusers et al., 1977; Chabert and Engeldinger, 1956; Ettema, 1980; Laursen & Toch, 1956; Tseng et al., 2000). It has been

discovered that the shape of the pier has an effect on the fluid-structure interaction at the upstream face of the pier, as well as the horseshoe and wake vortices. In an investigation using numerical simulations, Tseng et al. (2000) concluded that the extent of the wake and horseshoe vortices were larger and the position of the horseshoe vortex was further from the upstream face of the pier for square piers compared to circular cylinders. For sharp-nosed piers, no vorticity is created at the nose, although some vortex systems evolve, as expected around any bridge pier (Breusers et al., 1977). In scour depth estimation methods, pier shape is often taken into consideration by a pier shape factor ( $K_s$ ). Multiple pier shape factors have been proposed in the literature, often derived using the ratio of scour depth of circular piers to other shaped piers. Al-Shukur and Obeid (2016) took shape factors from different researchers, including Laursen and Toch (1956), Chabert and Engeldinger (1956), and Ettema (1980), and summarized their findings in one comprehensive table. Table 2.1 outlines various shape factors that have been proposed for the use of scour depth estimations.

*Table 2.1: Shape factors proposed for various pier shapes*

<b>Researcher(s)</b>	<b>Circular</b>	<b>Round-nosed</b>	<b>Sharp-nosed</b>	<b>Square-nosed</b>
Neill (1973)	2	2	3	1
Froehlich (1988)	1.0	1.0	0.7	1.3
Richardson and Davis (2001)	1.0	1.0	0.9	1.1
Al-Shukur and Obeid (2016)	1	0.85	0.7	1.11

The shape of the pier can also be characterized by the drag coefficient ( $C_D$ ), as  $C_D$  is dependent on the geometry of the body that the flow is encountering. In recent research, (Coscarella et al., 2020) followed the methodology used in Manes and Brocchini (2015) of examining the physical phenomenology to derive a new formula for scour prediction which mitigates the lack of clear physical basis found in empirical-derived formulae. The resulting equation for clear-water scour prediction included  $C_D$  as an input parameter and yielded more accurate scour estimations than those which did not include  $C_D$ .

#### **2.2.4 Flow Separation Velocity from Pier**

The flow separation velocity from the bridge pier,  $U_s$ , is not typically included as an input parameter in the development of scour estimation models. However, scour action is initiated at the point of separation on the pier face, making this velocity highly influential on scour depth. At the point of separation, the flow velocity reaches a maximum value, known as  $U_s$ . The flow separation velocity can be determined when the base pressure coefficient is known, as  $U_s$  is a function of base pressure on the pier's downstream face (Norberg, 1987; Roshko, 1961). Blockage effects can also be captured with the use of  $U_s$  as the pressure distribution around the pier is amplified with increasing blockage (Ramamurthy & Lee, 1973). When developing a scour estimation method, Williams (2016) introduced  $U_s$  as an input parameter to “describe the propensity of increased blockage to increase wall interference.”

### **2.3 Scour Estimation Methods**

In current industry practice, foundation design is based on approved code-specified methods with respect to bridge pier scour. These methods are typically empirical equations, developed by curve-fitting to experimental data. Many cautions have been proposed for the estimation of equilibrium scour depth, especially when extrapolating to field situations. Recent research shows that there are several deficiencies with current prediction equations, such as producing unnecessarily high estimates (Williams et al. 2013). Many challenges arise in developing an accurate equation with curve-fitting methods. These challenges include the complexity of the scour mechanism, the inability to quantify all scour influences, and the limitations of geometric and flow conditions. Additionally, scale effects of hydraulic modelling create difficulty in obtaining accurate experimental data.

### 2.3.1 Scour Depth Estimation

The current work will focus on four estimation methods, selected based on use in practice, applicability to current work and recentness of development. These equations include the Froehlich (1988) equation, HEC-18 (2001) equation, the Sheppard-Melville (2011, 2014) equation, and the Williams (2016) equation.

#### 2.3.1.1 Froehlich (1988) Equation:

The Froehlich equation was developed through regression of over 70 field data points to account for pier shape and angle of attack of approach flow. The equation is one of few which utilized field data rather than laboratory data for development:

$$\frac{d_{se}}{D} = 0.32K_{SF}Fr^{0.2} \left(\frac{D_P}{D}\right)^{0.62} \left(\frac{h}{D}\right)^{0.46} \left(\frac{D}{D_{50}}\right)^{0.08} + 1 \quad (2.4)$$

where  $D_P$  is the projected width of the pier and  $K_{SF}$  is the Froehlich pier shape factor.

#### 2.3.1.2 Colorado State University or HEC-18 (2001) Equation:

The most commonly used equation in scour depth estimation was published in the 1993 Hydraulic Engineering Circular No. 18 and is known as the Colorado State University (CSU) or HEC-18 equation. The original equation included three “K” factors to account for differing scour influences: angle of attack, bed condition and pier shape. The equation has since been modified by the inclusion of a fourth “K” factor to account for influence of bed material size causing an armoring condition:

$$\frac{d_{se}}{D} = 2.0K_sK_2K_3K_4\left(\frac{h}{D}\right)^{0.35} Fr^{0.43} \quad (2.5)$$

where  $K_s$  is the shape factor,  $K_2$  is the angle of attack factor,  $K_3$  is the bed condition factor and  $K_4$  is the armoring condition factor.

### 2.3.1.3 Sheppard-Melville (2011, 2014) Equation:

The Sheppard-Melville (S/M) equation was developed by melding and slightly modifying the Sheppard and Miller (2006) and Melville (1997) equations to form a new equation. The resulting equation accounts for interactions between structure, flow and sediment:

$$\frac{d_{se}}{D} = 2.5f_1f_2f_3 \quad (2.6a)$$

$$f_1 = \tanh\left[\left(\frac{h}{D}\right)^{0.4}\right] \quad (2.6b)$$

$$f_2 = \left\{1 - 1.2 \left[\ln\left(\frac{U}{U_c}\right)\right]^2\right\} \quad (2.6c)$$

$$f_3 = \left[ \frac{\left(\frac{D}{D_{50}}\right)}{0.4\left(\frac{D}{D_{50}}\right)^{1.2} + 10.6\left(\frac{D}{D_{50}}\right)^{-0.13}} \right] \quad (2.6d)$$

### 2.3.1.4 Williams (2016) Equation:

The Williams (2016) equation was recently developed at the University of Windsor by curve-fitting to laboratory data. As previously mentioned, the flow separation velocity from the pier,  $U_s$ , was introduced as an input variable to account for blockage effects. The equation also utilizes the densimetric Froude number,  $F_{ds}$  – calculated with the separation velocity – which is representative of flow-sediment interactions:

$$\frac{d_{se}}{D} = 1.010(F_{ds})^{-0.284} \left(\frac{h}{D}\right)^{0.325} \left(\frac{D}{D_{50}}\right)^{0.059} \quad (2.7a)$$

$$F_{ds} = \frac{U_s}{\sqrt{g(SG-1)d_{50}}} \quad (2.7b)$$

where SG is the specific gravity of bed material.

#### 2.3.1.5 Evaluation of Methods

Multiple researchers have investigated various common empirical equations used for scour prediction. Typically, these investigations result in indications that there is a need for an updated or improved equation for bridge foundation design (Ettema et al. 2011). Several investigations have compared the empirical formulae to experimental, or laboratory, data to evaluate their accuracy. Investigations have also taken place to investigate the accuracy of such equations with field data. Results from both types of investigations were reviewed for the current research.

Ettema et al. (2011) reviewed existing leading methods for bridge pier scour depth estimations, including the HEC-18 (2001) and S/M (2011) equations discussed above. As a result of this investigation, it was found that the HEC-18 equation inadequately reflects certain aspects of the pier scour process. It was also determined that the equation provides unreasonably large estimates for wide piers and its upper-bound estimate for live-bed conditions is too extreme. Evaluation of the S/M equation indicated that the equation reflects the scour process better than the HEC-18 equation. However, the S/M equation was found to have its own limitations, and further investigation with its applicability to field use was recommended.

An investigation of various scour depth prediction methods, including the Froehlich (1988), HEC-18 (2001) and S/M (2011) equations was conducted at the University of Windsor using graphical relations (Williams et al. 2013). It was found that, except for investigations which involved scale effects, each equation overpredicted the relative equilibrium scour depth. It was also concluded that the HEC-18 equation performed the best for large-scale tests.

Sheppard et al. (2014) gathered 23 scour estimation equations for evaluation with laboratory and field data, including all the equations discussed above, with the exception of the Williams (2016) equation. Results of this investigation indicated that some equations yielded negative or extremely large scour estimates which were considered “unreasonable”. It was concluded that the predictions from the S/M (2011) equation resulted in the least total error, as well as lower underprediction error when compared to the other equations evaluated. In addition, the HEC-18 wide-pier correction factor was evaluated. It was concluded that, although the wide-pier correction factor lowered the unreasonably large scour estimates for wide piers, this led to an increased number of underpredicted scour measurements for both laboratory and field conditions.

### 2.3.2 Scour Width Estimation

Unlike scour depth estimation methods, there are only a few scour width estimation methods. The most commonly used estimation method is an equation developed by Richardson and Abed (1993) and published in the Hydraulic Engineering Circular No. 18:

$$w_s = d_{se}(K_{ws} + \cot \phi) \quad (2.8)$$

where  $w_s$  is the top width of the scour hole from each side of the pier,  $d_{se}$  is the scour depth,  $K_{ws}$  is a factor relating the bottom width of the scour hole to the scour depth and  $\phi$  is the angle of repose of the bed material (ranging from about  $30^\circ$  to  $44^\circ$ ). However, for practical applications in water, a simplified equation was suggested:

$$w_s = 2.0d_{se} \quad (2.9)$$

### 2.3.2.1 Evaluation of Method

As previously mentioned, accurate scour width predictions are important for many different reasons when it comes to bridge foundation design. The accuracy of the scour width estimation equation was evaluated by plotting the predicted versus observed scour width values, which is presented in Figure 2.4. The estimated scour width was calculated for cases in which the scour depth value was known and unknown from laboratory results conducted by various researchers. In the case in which the scour depth is unknown, the value was estimated using the HEC-18 equation. As can be seen in the plot, the prediction equation (2.9) is fairly accurate when the scour depth is known. However, when the scour depth is not known, the equations accuracy is severely decreased, resulting in unnecessarily high estimates. Although the equation can predict the expected scour width well when the scour depth is known, design engineers are more interested in how the equation performs when the depth is unknown. This is due to the fact that the scour depth measurement is not known when foundation design is taking place. The inaccuracy of the HEC-18 scour depth equation is propagated and amplified when estimating the expected scour width.

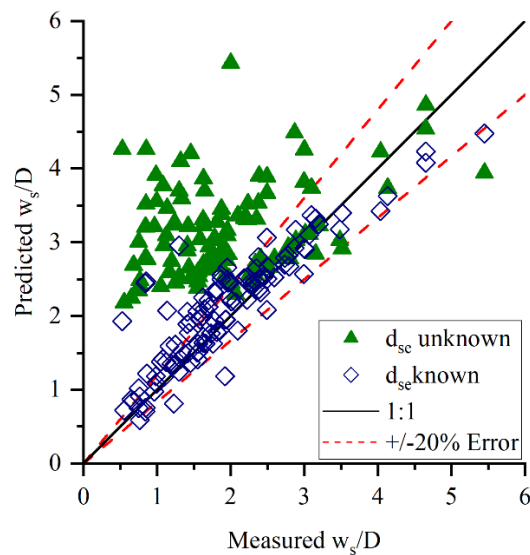


Figure 2.4: Predicted versus measured scour width values

## 2.4 Artificial Neural Networks (ANN)

ANNs are mathematical models that are devised from an analogy to brain cells and biological neural networks. As an artificial intelligence (AI) tool, ANNs can be applied in various fields and are capable of solving intricate problems such as optimization, simulation, estimation, and prediction, as well as model complex problems. Generally, ANN models consist of an input layer, hidden layer or layers, and an output layer. Nodes, also called neurons, make up each of these layers, with the number of nodes varying, depending on the development of the model. Both the number of nodes in the hidden layer(s) and number of hidden layers used are typically selected through trial and error. A general schematic of an ANN is illustrated in Figure 2.5. Input signals are received and summed (perhaps weighted) by the nodes, the sum is then passed through an activation function  $f$  and an output is generated. The output signals are then sent out to other nodes in the network. The resulting output variables of ANNs are produced by merging the connection weights with each input node after passing through an activation function.

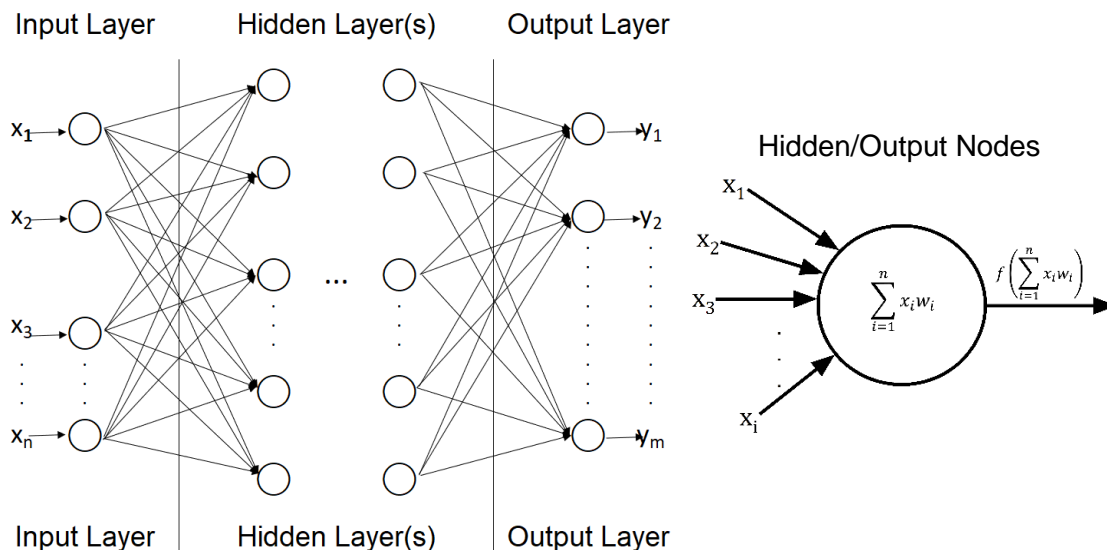


Figure 2.5: General schematic of an artificial neural network

Two data sets are used in the development of a neural network, a training data set and a validating data set. Typically, the training data set is larger than the validation set, but this is not necessary. The training data set is first used by the ANN to train the network; the network learns on this data to fit the model (i.e., weights and biases). Next, the validation data set is used to assess the performance of the network (i.e., the accuracy of the scour predictions). The performance of the networks is evaluated using a user-defined loss function which assesses the accuracy of the output(s) of the ANN. The validation data set provides an unbiased evaluation of the model fit while the model hyperparameters are being tuned. Finally, the testing data set can be used to evaluate the final, tuned network using data independent of that which it was trained on.

ANNs are composed of various hyperparameters that are manually set and must be tuned or optimized to ensure peak performance of the models. The model hyperparameters differ from the model parameters, as the parameters are automatically estimated from the data being used. ANN hyperparameters include number of hidden layers, number of nodes within the hidden layers, activation function, learning rate, optimizer, batch size and epochs.

Activation functions can be used to introduce non-linearity to the model. Three common activation functions applied to the scour problem are the sigmoid function, the hyperbolic tangent (tanh) function, and the rectified linear unit (ReLU) function, represented respectively as:

$$f(x) = \frac{1}{1+\exp(-x)} \quad (2.10)$$

$$f(x) = \frac{(e^x - e^{-x})}{(e^x + e^{-x})} \quad (2.11)$$

$$f(x) = \max(0, x) \quad (2.12)$$

where  $x$  is the known input vector.

Since ANNs employ a gradient descent algorithm, the learning rate is the step size taken to reach the minimum of the objective function. The learning rate is typically between zero and one and is evaluated and updated based on the behaviour of the loss function. The learning rate is one of the most important hyperparameters in a neural network. Learning rates that are too large can overshoot the minimum and can result in an unstable training process, while too small of a value can increase the length of the training process greatly and get stuck in a local minimum.

Epochs can be defined as the number of passes of the training data set the algorithm has completed or the number of trials the learning algorithm takes to learn from the input data. Batch size is the number of training data that is processed by the learning algorithm before the internal model parameters (i.e. weights and biases) are updated. The total number of iterations the model works through is the number of epochs multiplied by the number of batches. The ANN learns by reading the input data and applying various weights and calculations repeatedly, utilizing the results from the previous trials.

#### **2.4.1 ANNs and Scour Predictions**

Since the use of ANNs is a data-driven approach to solving problems, there are advantages to its use in the application of scour prediction over curve-fitting and linear regression. One main advantage is that no relationship between the input and output variables is assumed. Furthermore, the underlying physics of the problem does not need to be known. These aspects are favourable for the scour problem because of the complexity of the scour mechanism – despite the considerable body of work in this area over the past several decades, the scour process is not fully understood.

Many different approaches to development of ANNs for predicting equilibrium scour depth have been reported in literature. The development of the models varies by the types of ANNs, learning algorithms applied, and architecture of the network. Typically, the networks developed were simple back-propagation neural networks – ANNs with one hidden layer and limited hidden nodes employing a backpropagation learning algorithm. Backpropagation learning algorithms compute the gradient of the loss function from a forward pass and propagates it backward through the network to update the model. In general, the input parameters utilized in developing the ANN models have been based on governing parameters previously defined in the literature.

Choi and Cheong (2006) investigated the applicability of ANNs to predict local scour around bridge piers. The model was composed of normalized input parameters and trained on 64 sets of data from laboratory experiments. The model was tested with laboratory and field data separately. It was found that when tested on laboratory data, the model's predictions were fairly accurate. However, this accuracy was severely decreased when tested with field data. In an attempt to increase the accuracy of field estimations, the model was re-trained using field data. This model's accuracy was only increased slightly. In both cases, the model predictions were more accurate than the five empirical formulae they were tested against, thus concluding that ANNs can be applicable to the scour problem.

Bateni et al. (2007) evaluated an ANN model against an adaptive neuro-fuzzy inference system (ANFIS) and a radial-basis function network (RBF) for both equilibrium and time-dependent scour depth predictions. The neural network consisted of two hidden layers with 15 nodes within those layers and a tanh activation function. The input parameters were both normalized and scaled to a zero to one scale. The model was trained on 180 data sets from

laboratory experiment. It was concluded that, although the RBF network trained better and faster than the ANN, the ANN produced more accurate results compared to the ANFIS and RBF network.

In an investigation conducted by Toth and Brandimarte (2011), the influence of the experimental setting and sediment transportation mode on scour prediction with ANNs was analysed. The input variables for the models were dimensional and scaled so that the mean was equal to 0 and the variance was equal to one. Two large data sets were collected from field measurements and lab experiments. The data sets were then divided into subsets with increasing specialization degree, as shown in Figure 2.6. A network was developed for each set of data, totalling seven ANNs. Each network consisted of one hidden layer, with the number of nodes within the layers being optimized for each model. It was concluded that for the field data, there was no improvement in accuracy with increasing specialization, while an increase in accuracy with data set specialization was observed for the laboratory data, especially when going from all data to laboratory data only. Conversely, when tested with field data, the model trained on the full data set performed slightly better than the model trained on field measurements only.

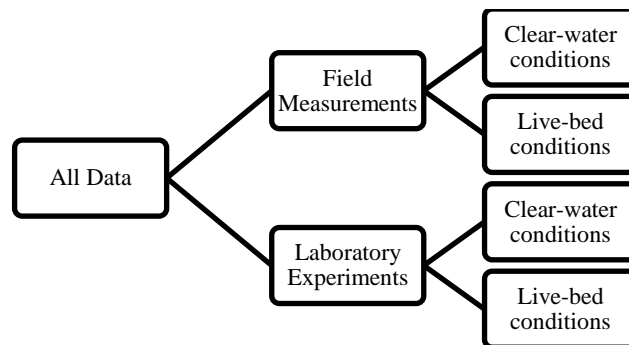


*Figure 2.6: Division of data sets in Toth and Brandimarte (2011) investigation*

Pal (2019) used a field data set to explore the applicability of deep neural networks (DNN) in bridge pier scour prediction. A DNN is a neural network with two or more hidden layers having

a large number of nodes and using sophisticated mathematical modelling. The model was developed using the ReLU activation function, dimensional input parameters and the adaptive moment estimation-based optimization algorithm (Adam). The resulting ANN consisted of three hidden layers with a varying number of nodes within each of the layers. When compared to a simple back-propagation neural network, the DNN produced more accurate results. A DNN with dropout layers was also developed, however there was no significant increase in accuracy between the DNN with and without dropout layers.

In an investigation conducted by Amini et al. (2020), the ability of an ANN to predict scour around complex bridge piers was evaluated. The model was developed using data from laboratory experiments and dimensional input parameters. The ANN consisted of one hidden layer with 3 nodes within that layer. When compared with the HEC-18 equation and the scour depth prediction equation for composite piers published in the Florida State Department of Transportation, the ANN produced more accurate scour estimations.

Since different approaches have been taken in the literature to reduce the data set, different input variables are taken for each prediction model. Table 2.2 outlines the input variables utilized in the investigations previously discussed. The table also consists of the input parameters from additional sources which developed field-trained neural networks. Although those ANNs which were trained on field data contained data for piers with varying shapes and L/D ratios, of the literature reviewed, only Toth and Brandimarte (2011) considered both shape factor and L/D in their model development. It is also important to note that none of the ANNs in the studies reviewed considered blockage effects in the development of the prediction models based on laboratory experiments. The inclusion of blockage ratio in such models may improve the performance of ANNs in predicting equilibrium scour depth.

Table 2.2: Input parameters utilized in literature for development of ANNs

Investigator(s)	Field Model Inputs	Laboratory-trained model Inputs
Choi and Cheong (2006)	Fr, D/h, $d_{50}/h$	Fr, D/h, $d_{50}/h$
Bateni et al. (2007)	N/A	$d_{50}$ , D, U, h, $U_c$
Lee et al. (2007)	$U/U_c$ , Fr, h/D, $d_{50}/D$ , $\sigma_g$	N/A
Toth and Brandimarte (2011)	D, U, h, $d_{50}$ , $K_2$ , $N_s^a$	D, U, h, $d_{50}$
Bonakdari and Ebtehaj (2017)	Fr, $d_{50}/h$ , D/h, L/h, $\sigma_g$	N/A
Pal (2019)	$K_s$ , D, $\theta$ , U, h, $d_{50}$ , $\sigma_g$	N/A
Shamshirband et al. (2020)	Fr, D/h, $d_{50}/h$ , $U/U_c$	$\sigma_g$ , D/h, $d_{50}/h$ , $U/U_c$

<sup>a</sup> Neill shape factor

In some cases, models were trained separately on field data and laboratory data. In each of the studies, the error values for the models trained on field data were significantly higher than those trained on laboratory data. There have been various rationales to the large variance in error values proposed. These include an increase of variation and paucity of field data compared to laboratory data. Field data tends to contain more noise which affects the training, and therefore the accuracy, of the models. There are many factors contributing to the noisiness of scour data obtained in field conditions, such as the uncontrolled nature of the field environment. When conducting scour experiments in a laboratory setting, the measurements are taken in a highly controlled environment. This type of control is not able to be replicated in the field. In addition, in laboratory conditions, the flume is typically emptied of the water before taking scour measurements. This allows for less interference while taking the measurements, as well as a clear indication of where the points of maximum scour depth and width are located, which is not achievable in field conditions. The channel itself may also have characteristics that are not able to be captured in the measurements, such as a bend in the channel upstream of the bridge pier(s). There lies a need for further research to increase the accuracy of field trained ANNs.

## CHAPTER 3

### SCOUR DATA

#### 3.1 Overview

As outlined in Section 2.4, machine learning models require a database to train, validate, and test the models. To develop a sufficient artificial neural network (ANN) to predict scour depth and width, existing scour data needs to be collated. For the current research, data from both laboratory experiments and field measurements were collected. The current chapter provides details of how the data was collected and analysed, and a discussion of the resulting data sets used to develop the networks.

#### 3.2 Laboratory Data

##### 3.2.1 Data Collection

To generate the laboratory database, data was collected from various sources around the world who have conducted scour experiments around bridge piers. The database consists of data which was extracted from publications, ranging from the years 1983 to 2021, and includes 70 data sets from the University of Windsor. A summary of resources and number of data sets from each source is outlined in Table 3.1. Data was obtained only from clear-water conditions around circular cylinder piers. In situations where the critical velocity of the bed material was not reported, the values were determined using the following formula (Melville & Sutherland, 1988):

$$\frac{U_c}{u_{*c}} = 5.75 \log \left( 5.53 \frac{h}{d_{50}} \right). \quad (3.1)$$

Here  $u_{*c}$  is the critical shear velocity, calculated using the following relationship (Melville, 1997):

$$u_{*c} = \begin{cases} 0.0115+0.0125(d_{50})^{1.4}, & 0.1 \text{ mm} < d_{50} < 1 \text{ mm} \\ 0.0305(d_{50})^{0.5}-0.0065(d_{50})^{-1}, & 1 \text{ mm} < d_{50} < 100 \text{ mm} \end{cases} \quad (3.2)$$

Table 3.1: Laboratory data resources

Investigator(s)	Year	Number of Data	Investigator(s)	Year	Number of Data
Raudkivi and Ettema	1983	12	Simarro et al.	2011	5
Yanmaz and Altinbilek	1991	32	Khwairakpam et al.	2012	12
Dey et al.	1995	18	Kothyari and Kumar	2012	3
Johnson and Torrico	1995	9	Lanca et al.	2013	34
Ahmed and Rajaratnam	1998	4	D'Alessandro	2013	19
Ettema et al.	1998	6	Tejada	2014	19
Melville and Chiew	1999	3	Aksoy and Eski	2016	28
Ting et al.	2012	5	Al-Shukur and Obeid	2016	3
Mia and Nago	2003	23	Williams	2016	22
Sheppard et al.	2004	12	Aksoy et al.	2017	16
Raikar and Dey	2005	20	Pandey et al.	2017	3
Grimaldi et al.*	2005	3	Khaple et al.	2017	2
Ettema et al.	2006	6	Link et al.	2019	14
Sheppard and Miller	2006	4	Pandey et al.	2020b	18
Lee and Strum	2009	3	Valela et al.	2021	6
Hodi	2009	9			

\*cited by Lanca et al. (2013)

Similarly, in cases where the Froude number was not reported, the values were determined using the equation:

$$Fr = \frac{U}{\sqrt{gh}} \quad (3.3)$$

Since an aspect of the current research is to explore the applicability of the flow separation velocity from the bridge pier as a potential velocity scale, it was required to determine the values of the flow separation velocity from the bridge pier for each case. The separation velocity was determined using a relationship proposed by Williams (2016):

$$k = 2.0649(D/B)^2 + 0.5264(D/B) + 1.4 \quad (3.4)$$

where  $k$  is the ratio of separation velocity to approach flow velocity (i.e.  $U_s/U$ ). The resulting separation velocity values calculated were also applied to equation (2.7b) to calculate the densimetric Froude number ( $F_{ds}$ ) incorporating  $U_s$ .

### 3.2.2 Resulting Database

The resulting laboratory database consists of 373 data points. A summary of the data collected can be found in Table 3.2. Matrix plots for the laboratory database are presented in Figure 3.1 for the dimensionless parameters presented in the summary table. Such plots allow for the visualization of the distribution of data and illustrates where data gaps may exist. A logarithmic scale was applied to the relative coarseness ( $D/d_{50}$ ) to achieve a clearer picture of the data distribution. A majority of the data falls between Froude numbers of 0.2 to 0.3, with significantly less data above a Froude number of 0.4. In terms of blockage ratio, a large percentage of the data falls below 10%; this is significant, as it has been previously reported that blockage effects do not affect scour below this threshold. Little data is present for flow shallowness ( $h/D$ ) over 3.5, with a significant data gap existing between  $h/D$  values of 10 to 15. The flow intensity values generally fall above a value of 0.8. In terms of relative coarseness, a majority of the data falls below 200, which is a value that is very rarely seen in field conditions unless the channel is a cobble- or boulder-bed stream. There is very little data with  $D/d_{50}$  values larger than 500, and there are many data gaps between a value of 500 and the maximum value of 4136. This distribution of relative coarseness values is one of the leading causes of scale effects in laboratory experiments of scour. The  $d_{se}/D$  values mostly fall between the values of 0.8 to 1.8, and generally follow a normal distribution.

Table 3.2: Statistical parameters for non-dimensional laboratory data

	<b>Fr</b>	<b>D/b</b>	<b>h/D</b>	<b>U/Uc</b>	<b>D/d<sub>50</sub></b>	<b>d<sub>se</sub>/D</b>
<b>Minimum</b>	0.044	0.0094	0.17	0.11	2.2	0.12
<b>Maximum</b>	0.75	0.25	16	0.99	4136	2.7
<b>Mean</b>	0.27	0.096	2.7	0.82	134	1.3
<b>Standard Deviation</b>	0.12	0.049	2.3	0.15	253	0.49

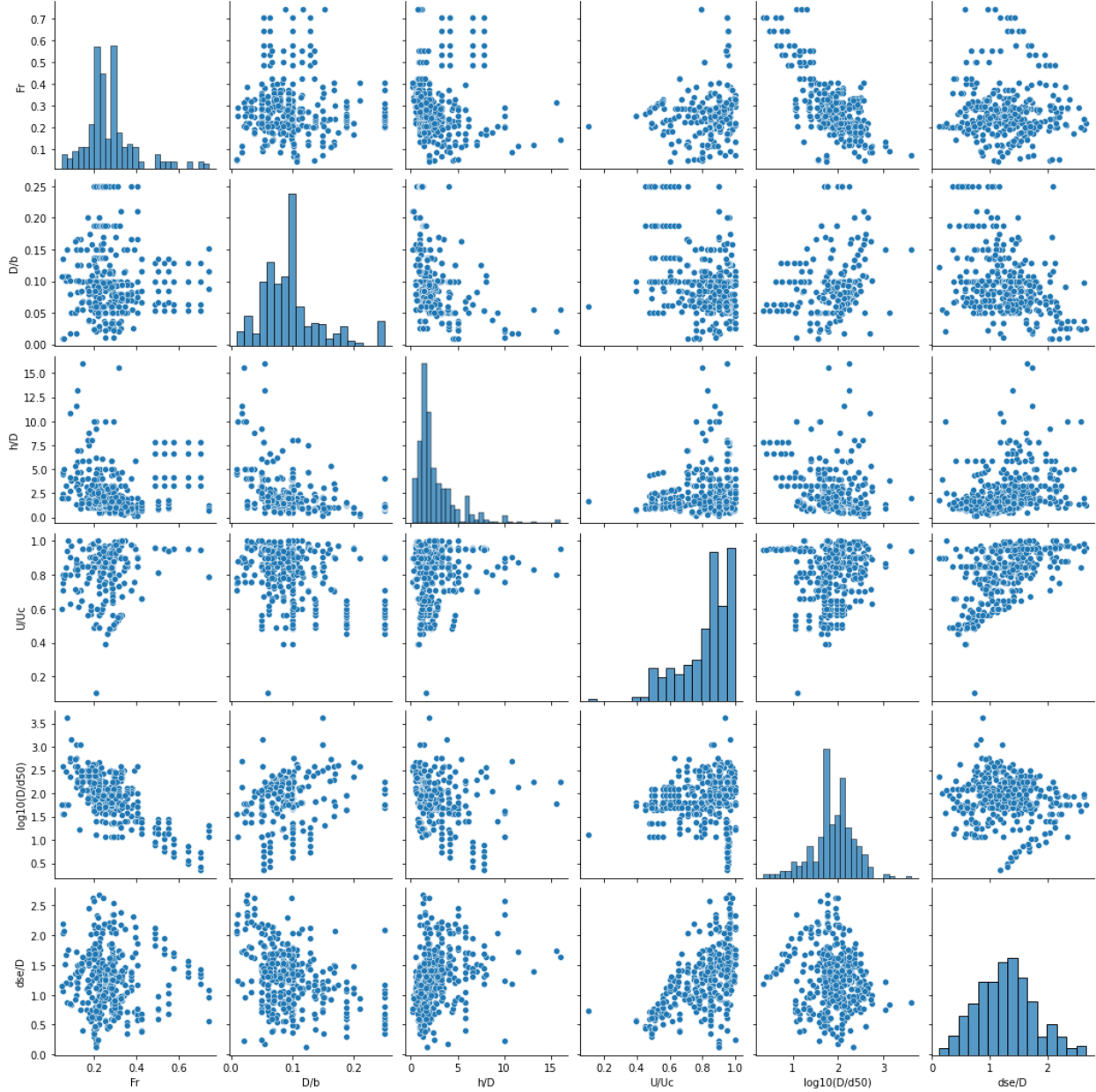


Figure 3.1: Pair-wise plots for non-dimensional laboratory data

### 3.2.3 Scour Width Data

Scour width data is not as commonly reported in the literature as scour depth values. As such, the scour width database consists of data only from the laboratory database which had complete data for scour width estimations. The resulting database consists of 110 data sets, including 70 sets from experiments conducted at the University of Windsor. A summary of the scour width database can be found in Table 3.3.

*Table 3.3: Statistical parameters for non-dimensional laboratory scour width data*

	<b>Fr</b>	<b>D/b</b>	<b>h/D</b>	<b>U/U<sub>c</sub></b>	<b>D/d<sub>50</sub></b>	<b>d<sub>se</sub>/D</b>	<b>w<sub>se</sub>/D</b>
<b>Minimum</b>	0.15	0.011	0.74	0.49	12	0.29	0.53
<b>Maximum</b>	0.55	0.25	10	0.94	236	2.4	6.4
<b>Mean</b>	0.27	0.10	2.3	0.77	85	1.1	1.9
<b>Standard Deviation</b>	0.094	0.055	1.7	0.13	54	0.42	1.0

### 3.3 Field Data

#### 3.3.1 Data Collection

The field database consists of field measurements collected from the United States Geological Survey (USGS) pier scour data (Benedict & Caldwell, 2014). The complete database includes data from 23 states and six other countries, including Canada, China, New Zealand, Nigeria, Russia and Yugoslavia. Although not all data includes the date on which the data was taken, of the dates that were recorded, the measurements have been obtained between the years of 1926 and 2007. The complete USGS pier scour database is quite expansive and includes data for a variety of conditions. Data from conditions which were not applicable to the ANN being developed here was discarded. This included data from grouped piers, piers at an angle to the approach flow, cohesive bed conditions, conditions with debris effects and measurements taken post flood. After these conditions were eliminated, the remaining data consisted of some

incomplete data sets (e.g. pier geometry information missing), which were also discarded from the database if the data was unable to be found elsewhere. Unlike the laboratory data, both live-bed and clear-water conditions were retained for the field database, as Toth and Brandimarte (2011) concluded that there was not an improvement in accuracy with increasing specialization of data (i.e. separation of live-bed and clear-water conditions).

Similar to the laboratory database, the  $U_c$  and  $U_s$  values were also calculated for the field data sets. The  $U_c$  values were determined using equation (3.1) presented in Section 3.2.1. The field data contained pier shapes other than round-nosed piers, so the separation velocity could not be obtained using equation (3.4), as the equation is only applicable to round-nosed piers. Hence, plots of  $k$  versus  $D/b$  for sharp-nosed, square-nosed, and round-nosed piers presented by Williams et al. (2019), as shown in Figure 3.2, were utilized to determine  $U_s$  values. The  $F_{ds}$  values were not calculated for the field database as the specific gravity of bed material was not reported, and it is unrealistic to assume the channel bed material is sand for all field conditions. In cases in which blockage information was not available, it was assumed that blockage effects were negligible. In cases in which the uniformity of particle size distribution ( $\sigma_g$ ) was not reported, it was assumed the bed material was uniform.

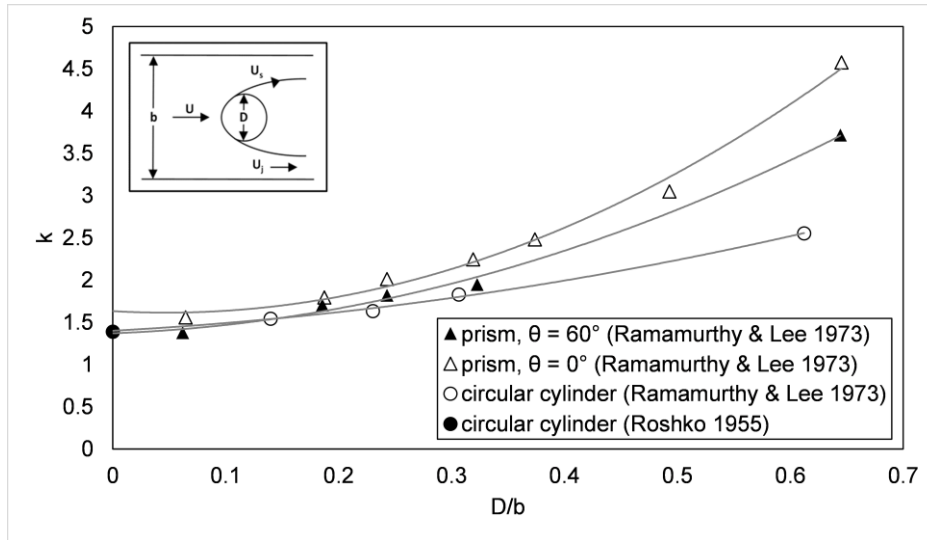


Figure 3.2: Variation of  $k$  parameter with blockage ratio and pier shape (extracted from Williams et al., 2019)

### 3.3.2 Final Database

The final database is made up of 329 data points. Table 3.4 outlines a summary of the non-dimensional parameters that make up the database. To further analyse the distribution of data, matrix plots for the field database are presented in Figure 3.3. A majority of the data sets have a Froude number of 0.375 or lower, with very few points having a Froude number greater than 0.5. Similar to what was observed with the laboratory data, a majority of the field data lies between  $h/D$  values of 1 and 3, with little data above a value of 6, with a data gap existing between the values of 10 and 15. Because both live-bed and clear-water conditions were retained for the field data, there is a much larger range of  $U/U_c$  values in the field data than the lab data. This will allow the network to be more versatile for field use. Within the field data, a larger number of data points with large  $D/d_{50}$  values are observed. The distribution of relative coarseness values is bimodal, with little data existing between the values of 100 and 700. The  $L/D$  values are left-skewed with little data existing over a value of 12, and a significant data gap exists between the values of 26 and the maximum value of 50. A majority of the  $\sigma_g$  values fall below 3, with many data gaps existing between the values 4 and 10. As was observed in the laboratory data, the

relative scour depth generally falls between the values of 0.8 and 1.8, with little data existing outside of this range.

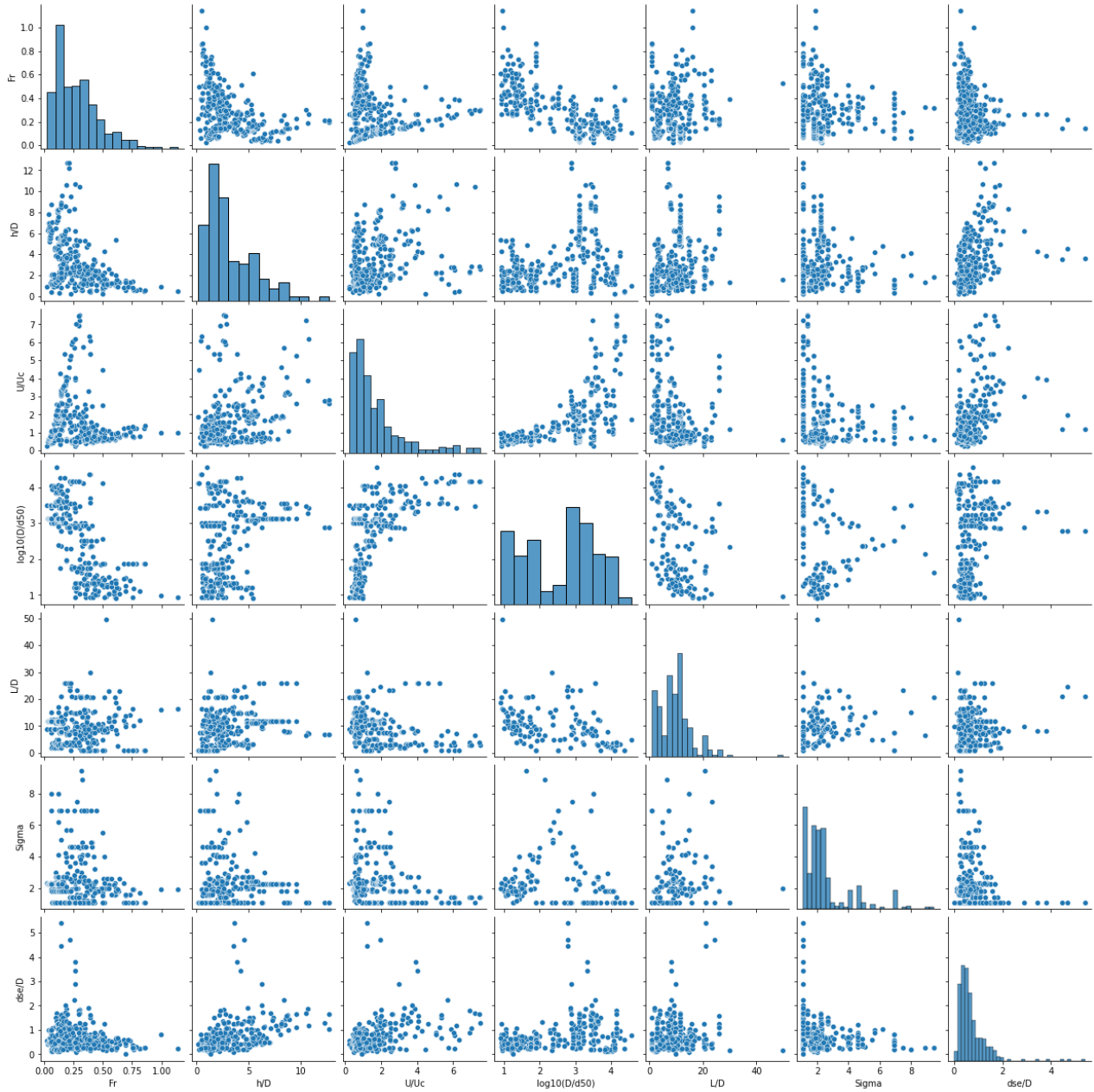


Figure 3.3: Pair-wise plots for non-dimensional field data

Table 3.4: Statistical parameters for non-dimensional field data

	<b>Fr</b>	<b>h/D</b>	<b>U/U<sub>c</sub></b>	<b>D/d<sub>50</sub></b>	<b>L/D</b>	<b>σ<sub>g</sub></b>	<b>d<sub>sc</sub>/D</b>
<b>Minimum</b>	0.03	0.18	0.24	8.1	1.00	1.2	0.10
<b>Maximum</b>	1.1	13	7.5	3657	50	9.4	5.4
<b>Mean</b>	0.29	3.2	1.7	2302	9.6	2.8	0.72
<b>Standard Deviation</b>	0.19	2.4	1.5	4345	6.1	1.5	0.63

### 3.4 Combined Dataset

A third database was also created using a combination of the laboratory and field databases outlined in Sections 3.2 and 3.3. However, the two databases were not simply combined to create one large database. Both the field and laboratory databases were analysed and reduced based on the  $D/d_{50}$  values. Field data with  $D/d_{50}$  values less than 200 were removed to eliminate cases of cobble-bed streams. Laboratory data were refined using the same minimum  $D/d_{50}$  value of 200, as this value does not exist in field conditions with sand or gravel bed material, and all laboratory experiments were conducted with either sand or gravel. As a result, 126 field sets and 313 lab sets were eliminated from the combination database.

#### 3.4.1 Final Database

The finalized combination database consists of 263 data sets, with 203 coming from field measurements and 60 from laboratory experiments. A summary of statistical parameters of the normalized parameters is outlined in Table 3.5. Matrix plots for the combination database were also created and are presented in Figure 3.4. Although some ranges of data are more populated than others within each parameter, there are no significant data gaps existing for the input values. One exception to this is at high (i.e.  $> 5$ ) gradation of particle size distribution values. The data gap that was present in the field database for relative scour depth also exists for the combination database.

The datasets outlined in the current chapter are to be applied to various scour prediction models in attempt to produce accurate scour depth and/or width estimations. A thorough understanding of the data being used in network development is important when generating an ANN, as ANNs require sufficient data to properly train and produce meaningful results. Knowledge of the databases being used to train a network is also crucial in understanding the limitations a model may have when applying it to data independent of the development dataset.

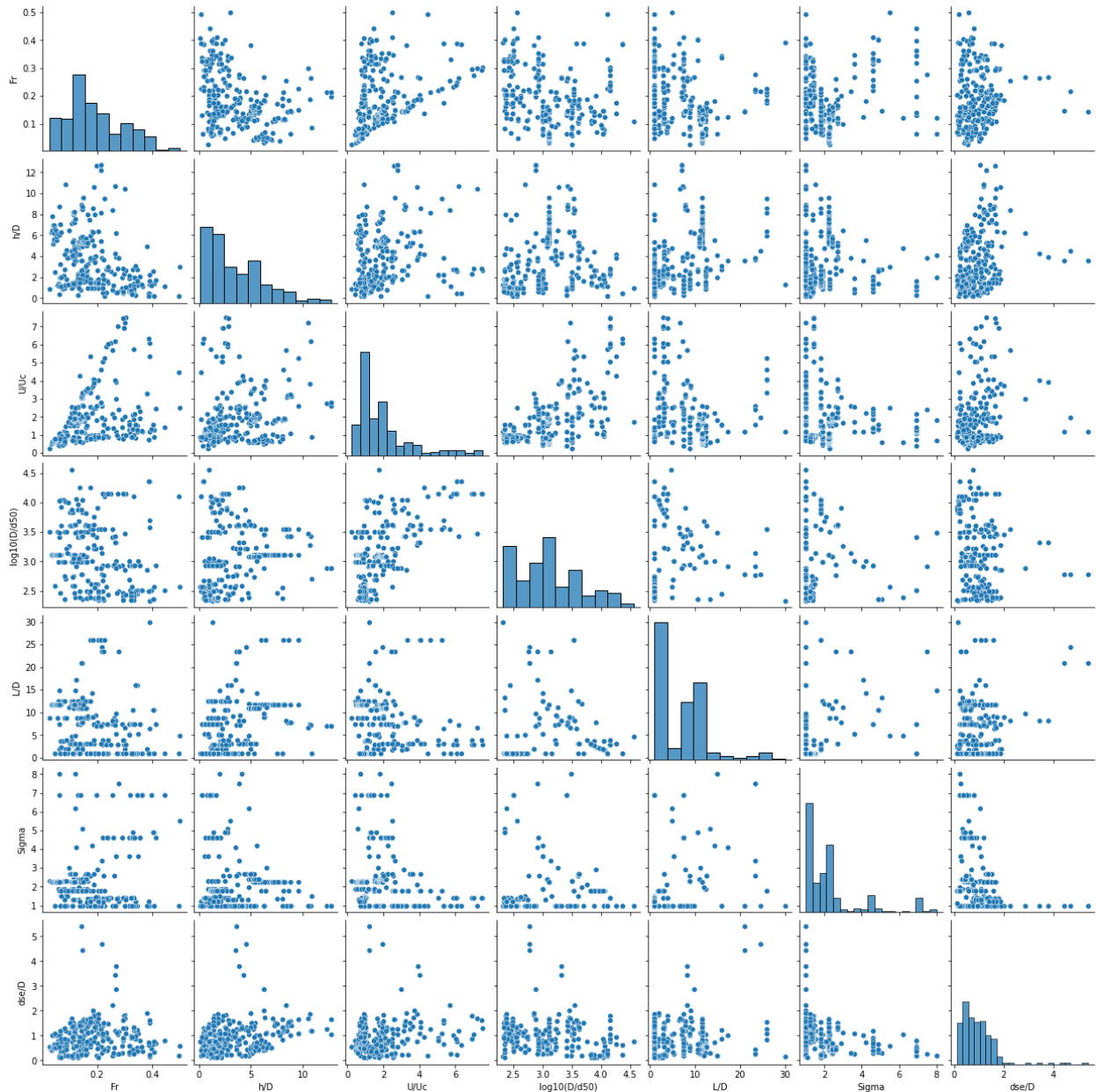


Figure 3.4: Pair-wise plots for non-dimensional combination data

Table 3.5: Statistical parameters for non-dimensional combination data

	<b>Fr</b>	<b>h/D</b>	<b>U/U<sub>c</sub></b>	<b>D/d<sub>50</sub></b>	<b>L/D</b>	<b>σ<sub>g</sub></b>	<b>d<sub>se</sub>/D</b>
<b>Minimum</b>	0.027	0.17	0.25	212	1	1.1	0.11
<b>Maximum</b>	0.50	13	7.5	36576	30	8.0	5.4
<b>Mean</b>	0.19	3.5	2.0	2960	7.0	2.3	0.93
<b>Standard Deviation</b>	0.010	2.7	1.5	4648	5.9	1.6	0.68

## CHAPTER 4

### MODEL DEVELOPMENT AND EVALUATION

#### 4.1 Model Development

The neural networks used in the current research were developed, trained, and tested using the PyTorch Lightning framework. The optimization algorithm selected was the adaptive moment estimation-based optimization algorithm (Adam) presented by Kingma and Ba (2017). Adam is used in place of classical stochastic gradient descent, as it computes individual adaptive learning rates for different parameters (Kingma & Ba, 2017), rather than maintaining a learning rate for each network weight. Adam is an effective and computationally efficient algorithm that is beneficial for noisy problems. The loss function for the ANNs was selected to be the mean squared error (MSE), given by the equation:

$$\text{MSE} = \frac{1}{n} \sum_{i=1}^n (y_i - \hat{y}_i)^2 \quad (4.1)$$

where  $n$  is the number of data points,  $y_i$  is the observed/actual value, and  $\hat{y}_i$  is the predicted value.

To become more familiar with the framework and optimization algorithm, a fictitious database was created based on equation (2.7), the scour depth prediction equation proposed by Williams (2016). The equation was used to develop a database similar to that which makes up the laboratory database and consisting of the same number of data sets as the laboratory database. Trial and error tests were run using the fabricated database to set some model hyperparameters, including batch size, number of epochs, and the train/validation/test data split. Through these tests, it was determined that a batch size of one produced the most accurate results, along with 150 epochs. It was also concluded that a random data split of 80% of the total

database used for training, 10% used for validation, and the remaining 10% used for testing was optimal. Based on these results, these hyperparameters were set for further development of the ANNs. It was also concluded that the default values for user-defined parameters within Adam were sufficient for the scour application, with the exception of the initial learning rate, which is to be optimized.

#### **4.1.1 Optimization of Hyperparameters**

The remaining hyperparameters to be tuned were optimized using the automatic hyperparameter software framework, Optuna (Akiba et al., 2019). Optuna differs from learning algorithms (i.e., Adam) as its purpose is to optimize the architecture of a network, while learning algorithms are used to train and update the network. When applying Optuna to an ANN, the use of a learning algorithm is required for the network to learn the dataset and update the model's weights and biases accordingly. The Optuna framework conducts studies of multiple trials to determine the optimal set of hyperparameter values. Within the Optuna framework, a study is defined as an optimization based on an objective function and a trial is defined as a single execution of the objective function. Each study conducted in the current research consisted of 50 trials, which was deemed sufficient for the current application. Two main user-defined parameters are required to run the optimization software: the sampler and pruning algorithm. Samplers are the algorithms used to continually narrow down the search space using the record of suggested parameter values and evaluated objective values, rather than utilizing a random search. Pruners automatically stop unpromising trials in the early stages of training to save computational costs. It was determined that the default parameters for the sampler were sufficient for the current application. The pruner selected to be utilized was the median pruner, which stops a trial when the best intermediate result is worse than the median of intermediate

results of previous trials. The pruner was applied such that it would not be enabled until after 30 epochs (i.e., 20% of total) had been completed to ensure each trial had sufficient time to train before being deemed unpromising. The hyperparameters optimized within the Optuna framework are outlined in Table 4.1, the range of values in which the hyperparameters were optimized were determined through a review of the literature and common practice in similar cases.

*Table 4.1: Hyperparameters optimized using Optuna framework*

<b>Parameter</b>	<b>Range</b>	<b>Search Type</b>
Number of hidden layers	1-5	Integer
Number of nodes within hidden layers	1-15	Integer
Learning rate	$1 \times 10^{-5} - 1$	Log Uniform
Activation function	ReLU, Sigmoid, Tanh	Categorical

Scaling methods for the input parameters were also investigated and validated in model development. Two different scaling methods, along with no scaling, were tested. The first scaling method resulted in each parameter's values falling within a range of zero to one. The second method resulted in each input parameter having a mean value of zero and a standard deviation of one. Respectively, the equations used to achieve the scaling are:

$$X_{iN} = \frac{X_i - X_{\min}}{X_{\max} - X_{\min}} \quad (4.2)$$

$$X_{iN} = \frac{X_i - \bar{X}}{\sigma} \quad (4.3)$$

where  $X_i$  is the input value,  $X_{\min}$  is minimum value of  $X$ ,  $X_{\max}$  is the maximum value of  $X$ ,  $X_{iN}$  is scaled input value,  $\bar{X}$  is the mean of  $X$  values, and  $\sigma$  is the standard deviation of  $X$  values. To determine which scaling method, if any, was optimal for each model, Optuna studies were conducted with each set of input parameters. The study which resulted in the lowest error value was selected for further analysis. Other hyperparameters, such as number of epochs, that were

selected based on the practice runs with a fictitious data set were verified and updated if necessary, once the optimized model was selected.

#### 4.1.2 Sensitivity Analysis

Sensitivity analysis was conducted on each of the optimized models to get an understanding of the influence of each individual input parameter on the models. The sensitivity analyses were conducted by repeating the model training process with each input parameter excluded (e.g., if a model originally has five input variables, it goes through the training process five additional times, each with a different input parameter missing). An example of the databases/input parameters that may be used in a sensitivity analysis is outlined in Table 4.2. The results from the model with parameters missing gives an understanding of how each parameter affects the model. Conducting a sensitivity analysis also allows for the selection of only the most effective parameters to be included in the model, improving the efficiency of the model.

*Table 4.2: Example input parameters used to conduct sensitivity analysis*

<b>Run</b>	<b>Missing Parameter</b>	<b>Input Parameters</b>
1	None	Fr, L/D, h/D, U/U <sub>c</sub> , D/d <sub>50</sub>
2	D/d <sub>50</sub>	Fr, L/D, h/D, U/U <sub>c</sub>
3	U/U <sub>c</sub>	Fr, L/D, h/D, D/d <sub>50</sub>
4	h/D	Fr, L/D, U/U <sub>c</sub> , D/d <sub>50</sub>
5	L/D	Fr, h/D, U/U <sub>c</sub> , D/d <sub>50</sub>
6	Fr	L/D, h/D, U/U <sub>c</sub> , D/d <sub>50</sub>

#### 4.2 Model Evaluation

For each of the databases discussed in Chapter 3, a set of testing data was created and utilized for all evaluation of the respective models developed using the different databases (i.e., the same data set was used for all evaluations of the laboratory-trained model, while a separate set of test data was utilized to conduct all the evaluations for the field-trained model). The accuracy of the ANN model predictions is primarily evaluated with the utilization of scatterplots of the predicted

versus measured scour values, as was done in Section 2.3.2.1 to evaluate the performance of the scour width prediction equation. These scatter plots include an exact-match line (i.e., the predicted value is the same as the measured value) and 20 percent error bounds. Error bounds of 20 percent was selected based on the evaluation of scour predictions and error bounds utilized in literature. Using the scatter plots, the performance of the models is assessed by how close the points fall to the exact-match line, how many points fall within the 20 percent error bounds and whether the scour parameters are being underestimated. However, additional statistical parameters were also used to aid in the evaluation of the models. These error values include the MSE (equation (4.1)), correlation coefficient (R), mean absolute percent error (MAPE), and mean absolute error (MAE). The formulae used to calculate these values are:

$$R = \frac{\sum_{i=1}^n (y_i - \bar{y})(\hat{y}_i - \bar{\hat{y}})}{\sqrt{\sum_{i=1}^n (y_i - \bar{y})^2 \sum_{i=1}^n (\hat{y}_i - \bar{\hat{y}})^2}} \quad (4.4)$$

$$MAPE = \frac{1}{n} \sum_{i=1}^n \frac{|y_i - \hat{y}_i|}{y_i} \times 100 \quad (4.5)$$

$$MAE = \frac{1}{n} \sum_{i=1}^n |y_i - \hat{y}_i| \quad (4.6)$$

where  $\bar{y}$  is the mean observed value and  $\bar{\hat{y}}$  is the mean predicted value.

## CHAPTER 5

### RESULTS

#### 5.1 Laboratory-trained Model

The first model developed in this research was a laboratory-trained model, trained on the laboratory database. The main purpose of developing a laboratory-trained model was to validate the procedures used in the current research for ANN development. As observed in various literature, neural networks are a good tool for scour prediction since no mathematical model needs to be assumed a priori and the exact relationship between variables does not need to be known, among other reasons. ANNs are able to produce relatively accurate scour estimations, particularly in laboratory applications. The results of a laboratory-trained model, developed using the methodology outlined in Chapter 4, can be used to validate the model development methods. The laboratory-trained model was also utilized to evaluate the inclusion of blockage effects as an input parameter for scour prediction models.

The input parameters selected for the model development were chosen based on those considered to have the greatest influence on equilibrium scour depth:

$$\frac{d_{se}}{D} = f\left(Fr, \frac{D}{B}, \frac{h}{D}, \frac{U}{U_c}, \frac{D}{d_{50}}\right). \quad (5.1)$$

Parameters such as pier shape, pier length, and pier orientation were not considered as input parameters since all laboratory data consisted of circular cylinders where the incoming flow is in line with the pier.

Once the optimization process was completed, the resulting ANN consisted of three hidden layers with five hidden nodes within those layers and a learning rate of  $2.0 \times 10^{-2}$ . It was also

concluded that the sigmoid activation function and scaling of the inputs such that the inputs fall within a range of zero to one produced the most accurate results. A plot of the predicted versus measured relative equilibrium scour depths can be found in Figure 5.1. As can be seen in the figure, a majority of the data falls within the 20% error bounds, with some points falling directly on the exact-match line. This indicates that the ANN is able to produce accurate scour estimations, validating the model development process.

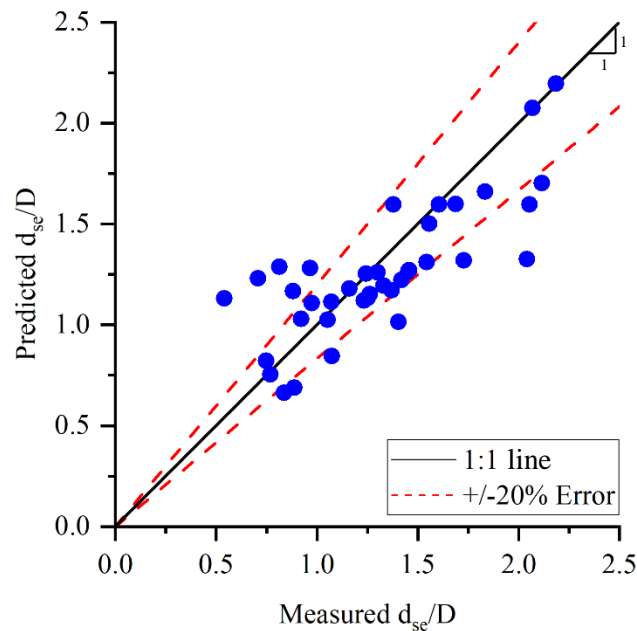


Figure 5.1: Predicted vs. observed  $d_{sc}/D$  for laboratory-trained model

### 5.1.1 Inclusion of Blockage Effects

In addition to validating the model development methodology, the laboratory network was utilized to analyse the inclusion of blockage effects in scour prediction. Initially, the model was re-trained and tested without the inclusion of blockage ratio as an input parameter. To analyse the influence of blockage effects, the optimization process was repeated without the input parameter  $D/B$ . Since the original network was optimized with  $D/B$  as an input parameter, simply removing the input from the model may not give a full understanding of how the blockage ratio affects the scour prediction in general. However, this method will give an idea of

how the blockage ratio affects the specific model that was originally developed. Repeating the optimization process allows the model to produce the most optimal results when blockage effects are not considered. The results from this analysis are presented in Table 5.1, where the minimum and maximum test error were determined using equations (5.2) and (5.3), respectively. As can be seen from the table, both the total loss and maximum error values increased with the exclusion of blockage effects.

*Table 5.1: Results from laboratory-trained ANNs including and excluding blockage effects*

<b>Model</b>	<b>Test Loss (MSE)</b>	<b>% Change</b>	<b>Min. Test Error</b>	<b>Max. Test Error</b>
With D/B	0.0724	-	$4.411 \times 10^{-5}$	0.5140
No D/B	0.1000	+38%	$3.460 \times 10^{-4}$	0.5624
Re-optimized No D/B	0.0978	+35%	$5.184 \times 10^{-5}$	0.5364

$$\text{Min. Test Error} = \min \left( (y_i - \hat{y}_i)^2 \right) \quad (5.2)$$

$$\text{Max. Test Error} = \max \left( (y_i - \hat{y}_i)^2 \right) \quad (5.3)$$

In addition to analysing the error values, the predicted versus measured relative equilibrium scour depth values were plotted and are presented in Figure 5.2. In both cases, the model was not able to make predictions as well as the model which included blockage effects. The models which did not include blockage effects had more points outside of the 20% error bounds and a small number of points on the exact-match line. It was also observed that the quality of estimations was decreased as the model gave the same prediction for various input conditions. The predictions from the models not including blockage effects may be less accurate because of the influence blockage effects have on scour hole geometry. As previously mentioned, even small changes in blockage can affect both the width and the depth of the scour hole. When blockage effects are not included in the model development, the model is missing an influential

parameter, potentially decreasing the ability of the scour prediction model to produce accurate results. These results validate previously mentioned investigations (D'Alessandro, 2013; Hodi, 2009; Tejada, 2014) which indicate that blockage effects have a significant effect on the equilibrium scour depth. As a result, blockage effects should be considered as an input variable when developing a scour prediction model for laboratory conditions.

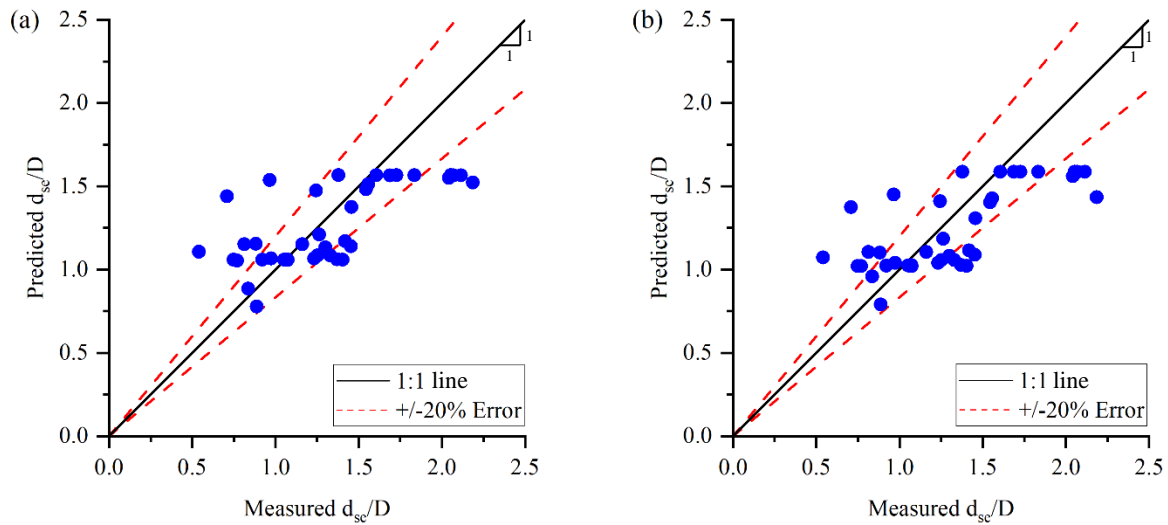


Figure 5.2: Predicted vs. measured  $d_{sc}/D$  for laboratory ANN (a) excluding  $D/B$  and (b) re-optimized without  $D/B$

### 5.1.2 Sensitivity Analysis

Results from the sensitivity analysis conducted on the laboratory-trained model are reported in Table 5.2. It was observed that the total error value increased with the exclusion of each input parameter. This indicates that each parameter selected had significant influence on the model. The flow intensity had the greatest influence, as the testing error increased the most when the  $U/U_c$  parameter was removed. Conversely, the flow shallowness value had the least influence on the model, as the error only increased by 18% after  $h/D$  was removed. It was also observed that the  $Fr$ ,  $D/B$ , and  $D/d_{50}$  parameters each had relatively the same impact on the prediction model. Results of the sensitivity analysis indicate that each input parameter that was initially selected has significant influence on the scour predictions and should be retained in the model.

Table 5.2: Sensitivity analysis results for laboratory-trained ANN

Missing Parameter	Test Loss (MSE)	% Change	Min. Test Error	Max. Test Error
None	0.0724	-	$4.411 \times 10^{-5}$	0.5140
Fr	0.1008	+39%	$1.543 \times 10^{-8}$	0.7165
D/B	0.1000	+38%	$5.095 \times 10^{-5}$	0.5361
h/D	0.0853	+18%	$4.731 \times 10^{-5}$	0.4281
U/U <sub>c</sub>	0.1542	+113%	$4.517 \times 10^{-7}$	0.8070
D/d <sub>50</sub>	0.0998	+38%	$1.354 \times 10^{-4}$	0.5164

### 5.1.3 Comparison to Prediction Equations

Further analysis on the accuracy of the ANN's equilibrium scour depth predictions was conducted with a comparison to the predictions using the equations discussed in Chapter 2, using the error values outlined in Chapter 3. A summary of these values is presented in Table 5.3. In each of the error values calculated, the ANN produced the most favourable result. It was observed that the error values from the ANN were significantly more favourable than the HEC-18 equation, which is the equation most commonly used in practice. Plots of predicted versus measured relative equilibrium scour depth values were also created for analysis and are presented in Figure 5.3. From these plots it is evident that the equilibrium scour depth predictions produced from empirical formulae do not achieve the same level of accuracy as the ANN. Each of the equations produced a higher percentage of data falling outside of the 20% error bounds than the current ANN model. It is also observed that the S/M (2011) equation produced the least accurate predictions, while the Williams (2016) equation produced the most accurate results.

Table 5.3: Comparison of laboratory ANN to empirical formulae

Model	ANN	Froehlich (1988)	HEC-18 (2001)	S/M (2011)	Williams (2016)
MSE	0.0724	0.1771	0.4226	0.4442	0.2024
MAE	0.2023	0.3441	0.4916	0.5749	0.3381
MAPE	18%	33%	44%	56%	22%
R	0.7877	0.4905	0.3784	0.3963	0.5161

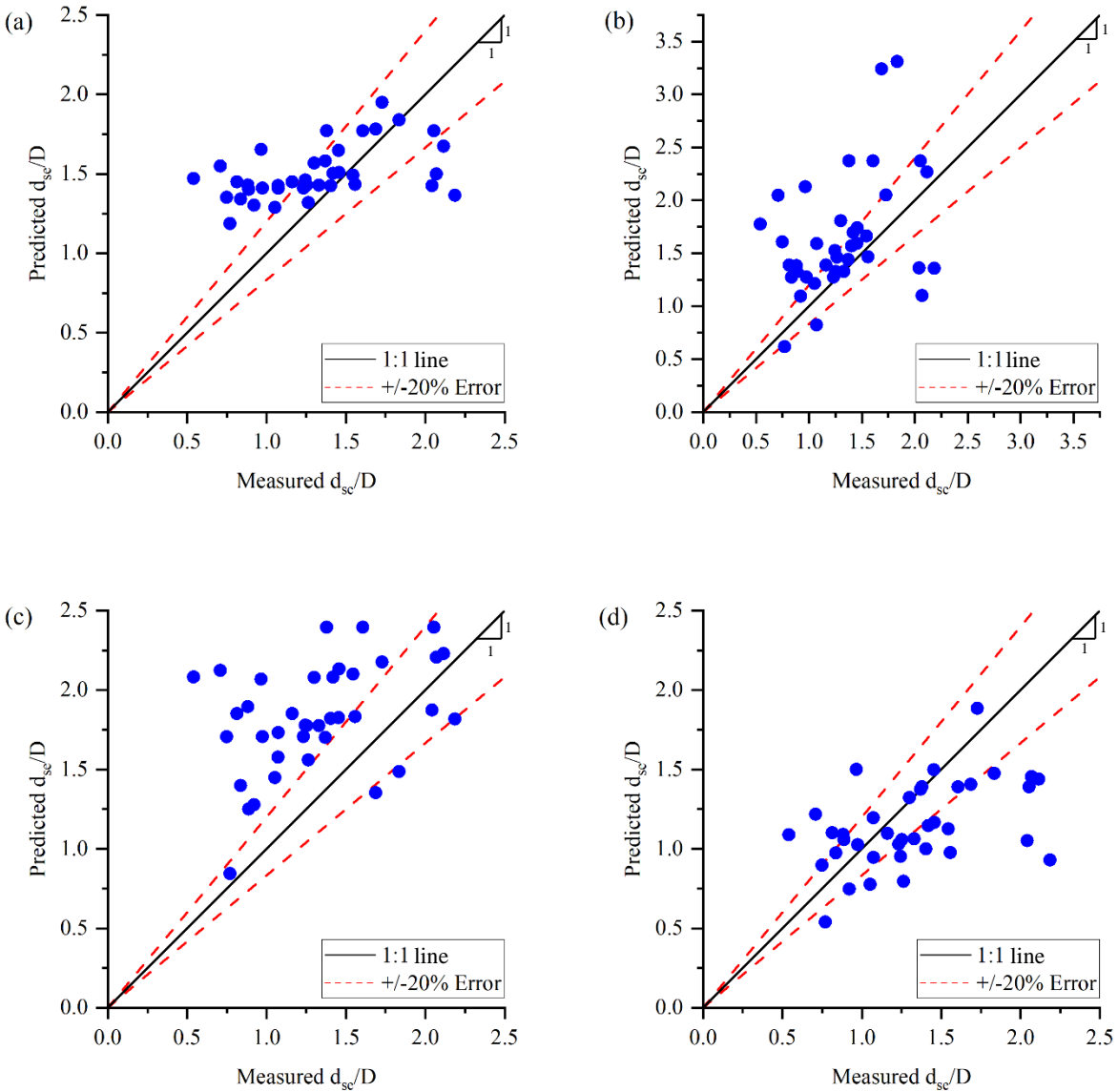


Figure 5.3: Predicted versus observed  $d_{sc}/D$  for the (a) Froelich (1988) equation, (b) HEC-18 equation, (c) S/M (2011) equation, and (d) Williams (2016) equation applied to laboratory data

### 5.1.4 Field Estimations

The final analysis conducted on the laboratory-trained ANN was to evaluate the model's applicability to field scour estimations. To complete this analysis, the field data which fit the criteria on which the laboratory database was created (e.g., circular cylinders) were retained and applied to the model. The results of the predicted versus measured  $d_{sc}/D$  values from the field

data are presented in Figure 5.4. It is evident from this plot that the laboratory-trained model is unable to produce meaningful scour estimations from field data. This supports the idea that scour prediction models developed solely on laboratory data do not translate well to field use. There are many reasons why a laboratory-trained model would be ineffective in field use, including the scale effects that are present during laboratory experimentation. There are also parameters that occur in the field that lie outside of the range that is achievable through laboratory experimentation, leaving aspects of field scour development out of consideration when developing these scour prediction models. This reiterates the need for an accurate scour prediction model developed from field-based data.

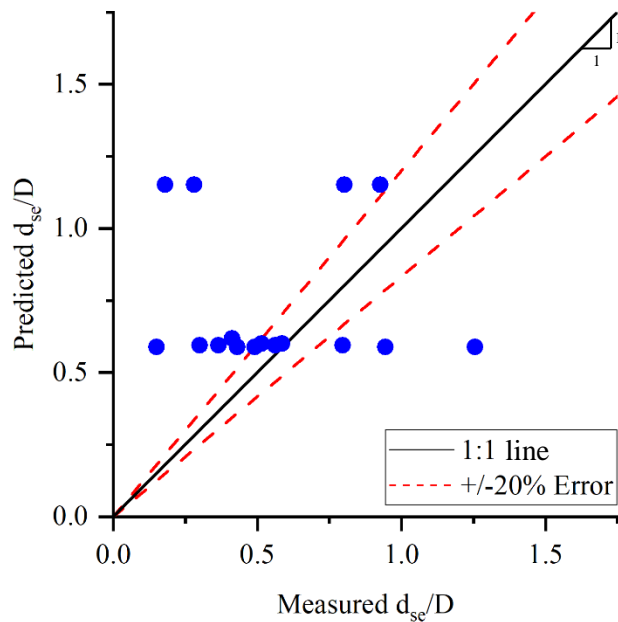


Figure 5.4: Predicted vs. measured  $d_{sc}/D$  for field scour estimations produced from the laboratory-trained ANN

## 5.2 Field Model

Similar to the laboratory-trained model, a field-trained model was developed following the procedure outlined in Chapter 4, with a set of input parameters selected based on those which

have greatest influence on equilibrium scour depth. For the field-trained model, the specific set of input parameters for the ANN are chosen as:

$$\frac{d_{sc}}{D} = f\left(\text{Fr}, \frac{h}{D}, \frac{U}{U_c}, \frac{D}{d_{50}}, \frac{L}{D}, K_S, \sigma_g\right) \quad (5.4)$$

where  $K_S$  is the HEC-18 shape factor. Since the field database is made up of data from conditions in which the pier is in line with the approach flow, the pier orientation was not considered an input variable. Unlike the laboratory data, the field database also consists of non-circular piers with varying aspect ratios ( $L/D$ ), leading to the inclusion of both a pier shape factor and  $L/D$  as input parameters. The field data also consist of data for conditions in which the bed material is not uniform (i.e.,  $\sigma_g > 1.5$ ), hence the inclusion of  $\sigma_g$  as an input parameter.

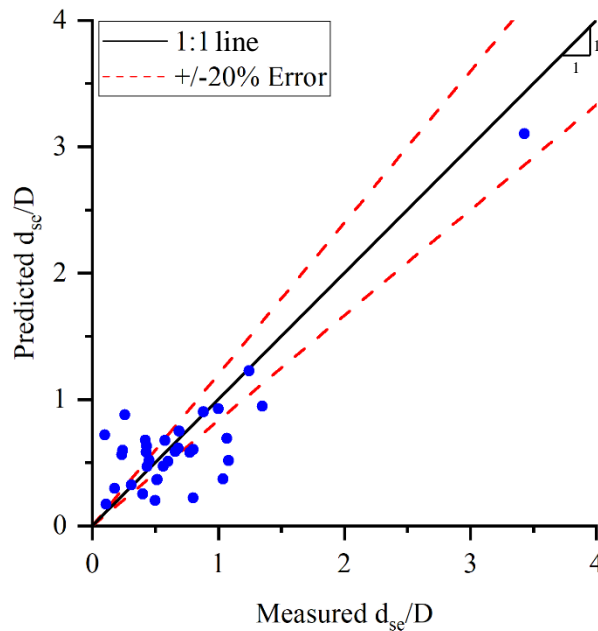


Figure 5.5: Predicted vs. actual  $d_{sc}/D$  for field-trained ANN

The optimized ANN consisted of one hidden layer with 13 nodes within that layer and a learning rate of  $2.8 \times 10^{-3}$ . The network utilized the sigmoid activation function and a scaling method in which the mean of the inputs is equal to zero with a variance of one. It was also observed that increasing the number of epochs from 150 to 200 resulted in more accurate

predictions. Increasing the number of epochs any further resulted in some negative values for the scour predictions. A plot of predicted versus measured  $d_{se}/D$  values from the optimized model is shown in Figure 5.5. From this plot it is observed that although the estimations are relatively accurate, a larger percentage of the data falls outside of the 20% error bounds than what was observed in the laboratory estimations.

### 5.2.1 Shape Factors

As discussed in Section 2.2.3, there have been many different pier shape factors proposed for scour predictions, typically derived by using the ratio of scour depth for circular piers to other shaped piers. As previously discussed, the pier shape could be characterized by the drag coefficient ( $C_D$ ), which was introduced to the scour problem to improve the physical basis of scour prediction models (Coscarella et al., 2020). In an effort to improve the field equilibrium scour depth estimations, an ANN was optimized with the physics-based parameter,  $C_D$ . Additionally, ANNs were optimized with the Neill (1973) shape factors and Al-Shukur and Obeid (2016) shape factors (A&O), outlined in Table 2.1, for comparison. The results from these models are presented in Table 5.4. From this table, it can be seen that the total test error was decreased by 10% with the model using  $C_D$  as opposed to the HEC-18 shape factor. It is also evident that other empirical shape factors proposed do not improve the accuracy of scour predictions. To further analyse the applicability of  $C_D$ , the predicted versus measured relative equilibrium scour depth plot from this model is presented in Figure 5.6. The predicted versus measured  $d_{se}/D$  plots for the Neill and A&O models can be found in Appendix B. As evident from the plot, the scour predictions are closer to the agreement line than as seen with the HEC-18 model. It is also observed that the outlier point also falls closer to the exact-match line, indicating that the  $C_D$  model performs better for a wider range of data. These results indicate that physics-

based parameters, such as the pier drag coefficient, are more valuable than empirical values when applied to scour prediction models. Due to its benefits over the HEC-18 model, the  $C_D$  model was retained for further analysis. This ANN has the same structure as the HEC-18 model, with the exception of the learning rate, which was optimized as  $3.3 \times 10^{-3}$ .

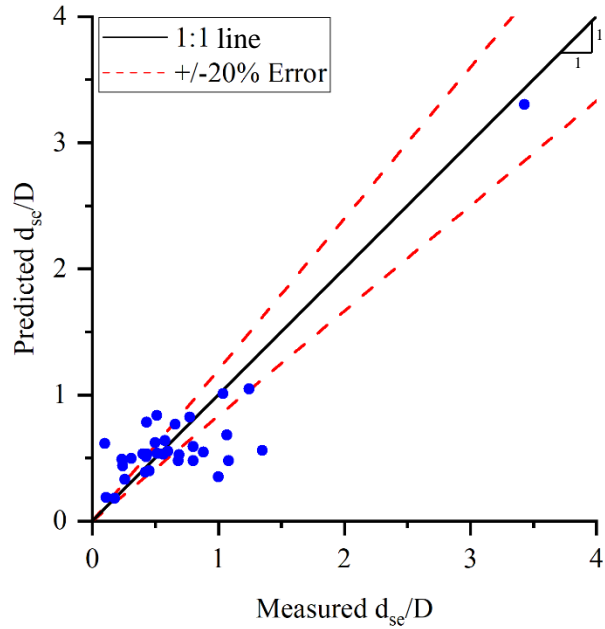


Figure 5.6: Predicted vs. observed  $d_{sc}/D$  for field-trained ANN with  $C_D$

Table 5.4: Results from applying different shape factors to the field-trained ANN

Shape Factor	Test Loss	% Change	Min. Test Error	Max. Test Error
HEC-18	0.0891	-	$1.298 \times 10^{-4}$	0.4455
$C_D$	0.0803	-10%	$6.618 \times 10^{-6}$	0.6228
Neill	0.0899	+1%	$3.087 \times 10^{-5}$	0.3946
A&O	0.1028	+15%	$2.375 \times 10^{-6}$	3.9447

### 5.2.2 Inclusion of Flow Separation Velocity

The applicability of  $U_s$  was also evaluated as a velocity scale for field-based scour prediction models. A new model was optimized with the flow separation velocity being introduced to the model in the form of the  $k$  value, where  $k$  is the flow separation velocity divided by the approach flow velocity (i.e.,  $k = U_s/U$ ). A second model was optimized with the separation velocity

divided by the critical velocity of the bed material (i.e.,  $U_s/U_c$ ). The results of these models, compared to those from the model utilising  $U/U_c$  as the velocity scale, can be found in Table 5.5. It is observed that the total error increases with the two different input parameters incorporating  $U_s$  compared to the model which uses  $U/U_c$  as the velocity input. This indicated that the flow intensity is the most efficient velocity scale parameter to apply to a scour prediction model based on field data. The separation velocity may not have a significant impact on the field-trained model as  $U_s$  was introduced to scour prediction by Williams (2016) to incorporate blockage effects. However, it was assumed that blockage is minimal in the field environment, making blockage effects negligible. The predicted versus measured  $d_{se}/D$  plots for the models including  $U_s$  can be found in Appendix B.

*Table 5.5: Comparison of field-trained ANNs with varying velocity scales*

<b>Velocity Scale</b>	<b>Test Loss (MSE)</b>	<b>% Change</b>	<b>Min. Test Error</b>	<b>Max. Test Error</b>
$U/U_c$	0.0803	-	$6.618 \times 10^{-6}$	0.6228
$k = U_s/U$	0.1023	+27%	$3.891 \times 10^{-4}$	0.8839
$U_s/U_c$	0.0893	+11%	$1.099 \times 10^{-5}$	0.6193

### 5.2.3 Sensitivity Analysis

The results obtained from the sensitivity analysis conducted on the field-trained ANN are presented in Table 5.6. From this table, it is observed that the error value increases with the exclusion of each of the input parameters, indicating that all parameters selected had a beneficial effect on the model. The  $h/D$ ,  $D/d_{50}$ ,  $L/D$  and  $\sigma_g$  input parameters all have significant value to the model, as the error increased by over 100% after each of these input parameters were removed. Of these parameters, the flow shallowness had the most significant impact on the model, with the largest increase in error. It is important to note that the  $L/D$  parameter had the second largest increase in error when excluded, although all data consisted of conditions where the pier is in line with the flow. This contradicts assertions in the literature that the aspect ratio does not have an effect on scour depth in these conditions. It is also observed that the maximum error

increases significantly with the exclusion of the  $h/D$ ,  $U/U_c$ ,  $D/d_{50}$ ,  $L/D$  and  $\sigma_g$  parameters, further emphasizing the importance of these parameters in this model. Additionally, the  $C_D$  parameter had the least impact on the model, with an increase of only eight percent, and a decrease in maximum error. However, the increase in total error value indicates that, although not as significant as the other parameters, the  $C_D$  parameter does add value to the model.

*Table 5.6: Sensitivity analysis results for field-trained ANN*

<b>Missing Parameter</b>	<b>Test Loss (MSE)</b>	<b>% Change</b>	<b>Min. Test Error</b>	<b>Max. Test Error</b>
None	0.0803	-	$6.618 \times 10^{-6}$	0.6228
Fr	0.1515	+89%	$1.543 \times 10^{-4}$	0.8549
$h/D$	0.1806	+125%	$1.592 \times 10^{-4}$	1.1426
$U/U_c$	0.1263	+57%	$8.305 \times 10^{-7}$	1.6571
$D/d_{50}$	0.1689	+110%	$1.820 \times 10^{-8}$	1.3541
$L/D$	0.1769	+120%	$2.737 \times 10^{-5}$	1.4882
$C_D$	0.0869	+8%	$3.964 \times 10^{-5}$	0.5001
$\sigma_g$	0.1697	+111%	$5.531 \times 10^{-5}$	1.1757

#### 5.2.4 Comparison to Equations

Similar to the laboratory-trained model, the predictions produced from the field-trained ANN were compared to those from commonly used formulae. The results of this analysis is outlined in Table 5.7. It is evident from the error values that the ANN produces the most accurate equilibrium scour depth estimations compared to each of the equations. Each of the MSE, MAE and MAPE values are significantly reduced in the ANN model compared to the HEC-18 equation. Additionally, the R value of the ANN model is approximately four times better than that of the HEC-18 equation. In addition to the error values, the predicted versus measured relative equilibrium scour depth values were plotted and presented in Figure 5.7. As observed with the laboratory scour predictions, it is apparent from the plots that the equations are not able to predict equilibrium scour depth to the same degree of accuracy of the neural network. It is observed that application of the equations to field data results in poorer equilibrium scour depth

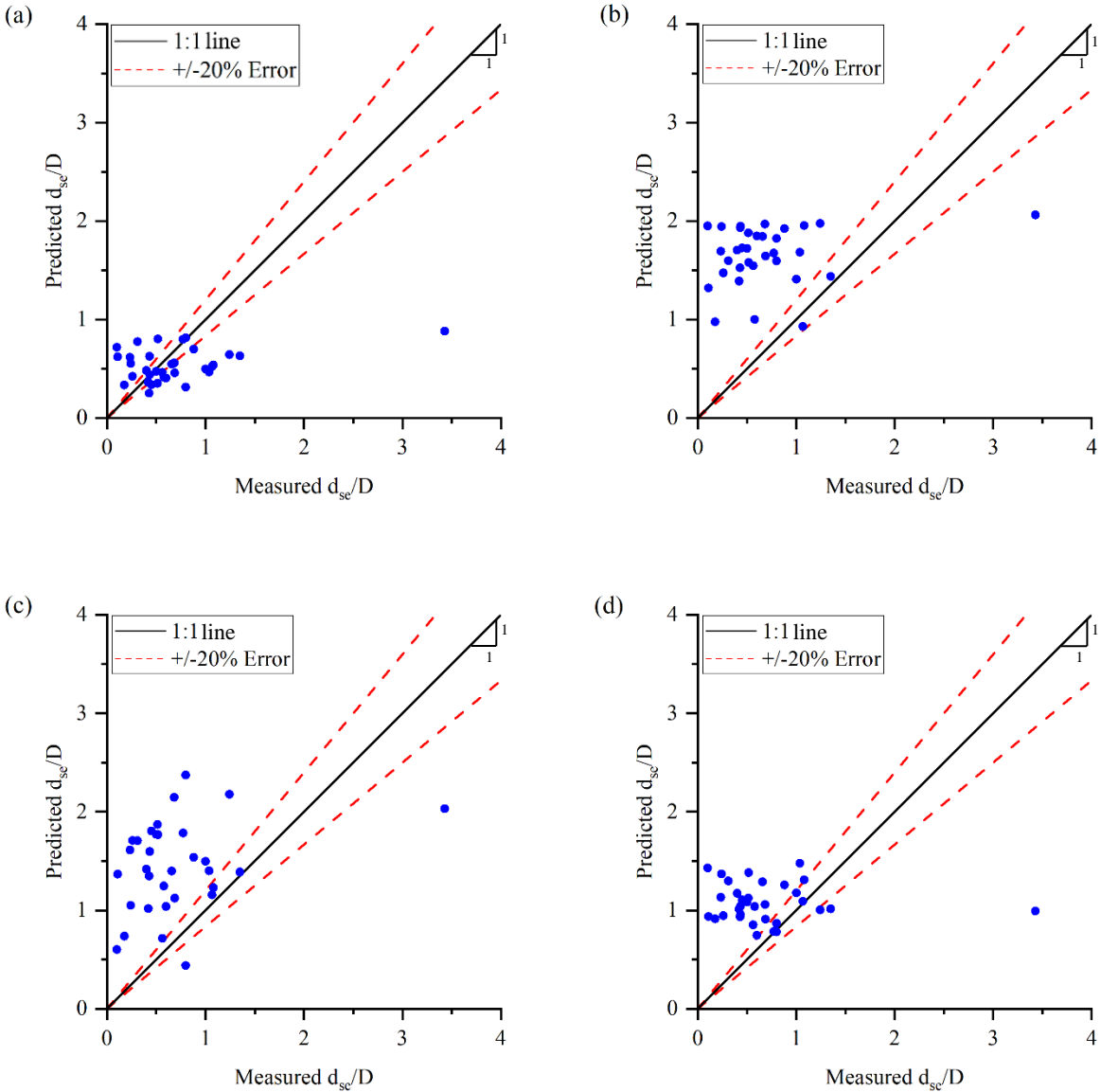


Figure 5.7: Predicted versus observed  $d_{sc}/D$  for the (a) Froelich (1988) equation, (b) HEC-18 equation, (c) S/M (2011) equation, and (d) Williams (2016) equation applied to field data

predictions than when applied to laboratory data. It is important to note that application of the S/M (2011) equation to the data resulted in some non-physical negative scour depth estimations which are not pictured in the plot. Although the error values and general predictions are significantly improved using the ANN compared to the empirical equations, there remains a desire for more accurate estimations. There is a larger percentage of datapoints falling outside of

the 20% error bounds on the field-trained plot than the laboratory plot, and there is a significant increase in MSE and MAPE values.

*Table 5.7: Comparison of error values from field ANN against empirical formulae*

<b>Error</b>	<b>ANN</b>	<b>Froelich (1988)</b>	<b>HEC-18 (2001)</b>	<b>S/M (2011)</b>	<b>Williams (2016)</b>
MSE	0.0803	0.3123	1.281	1.893	0.5360
MAE	0.2064	0.3442	1.059	1.018	0.5692
MAPE	48%	77%	300%	200%	176%
R	0.8756	0.3806	0.2263	-0.4374	-0.0727

### 5.3 Combined Model

In attempt to increase the accuracy of the field predictions, a model was trained on the combination database discussed in Section 3.4. This database is mainly composed of field data (77%), but also includes laboratory data to assist the ANN in learning and developing a more accurate scour prediction model. The input parameters used for this model were selected to be the same as those used in the field model (Equation (5.4)), with the exception of the pier shape factor. The drag coefficient was selected as the parameter to describe pier shape based on the results from the field-trained model. The optimized ANN was made up of one hidden layer with eleven nodes within that layer and a learning rate of  $6.7 \times 10^{-3}$ . This structure is very similar to that which was optimized for the field-trained model, with the learning rate being doubled. The optimal activation function was determined to be the sigmoid function and the optimal scaling method was that which results in the inputs falling within a range of zero to one. Similar to that observed with the field-trained network, the current network performed optimally with 200 epochs, rather than the originally selected 150 epochs. The plot of predicted versus measured  $d_{se}/D$  values is presented in Figure 5.8, where 77% of the data comes from field measurements. From this figure, it is observed that a majority of the data falls within the 20% error bounds, with

multiple points falling on the line of exact match. In general, the predictions from the current model are significantly more accurate than those from the field-trained model.

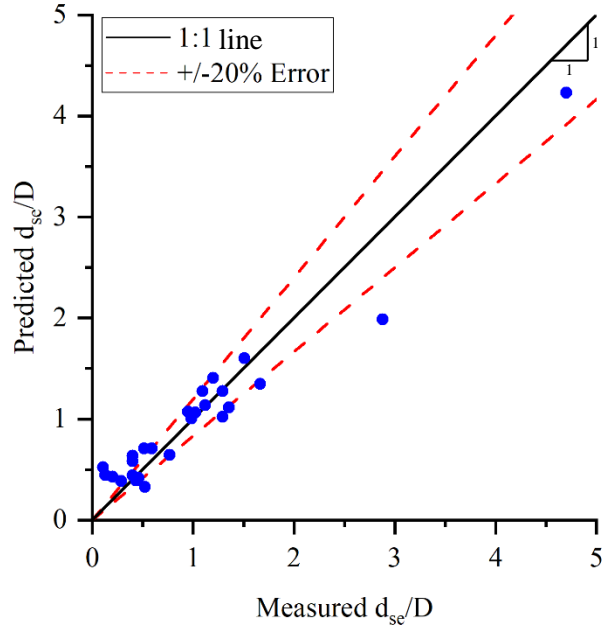


Figure 5.8: Predicted vs. measured  $d_{sc}/D$  for combination ANN

### 5.3.1 Shape Factors

To validate the selection of  $C_D$  as the parameter to incorporate pier shape, models were also optimized using the HEC-18, Neill and A&O shape factors. The results from these models are presented in Table 5.8. The predicted versus measured  $d_{sc}/D$  plots from the models with empirical shape factors can be found in Appendix B. As evident in the table, the total loss increases by at least 100% from the model with  $C_D$  to the models with the empirical shape factors. It is also observed that in all cases, especially those of the Neill and A&O shape factors, the maximum error also increases significantly. This large increase in maximum error resulted from the models being unable to accurately predict the scour depth for the outlier point (i.e., measured  $d_{sc}/D = 4.7$ ), indicating that these models cannot perform for a range of data over

which the  $C_D$  model is capable of. This further supports the selection of the parameter  $C_D$  to describe pier shape in the scour prediction models.

*Table 5.8: Results of applying various shape factors to combined-trained model*

<b>Shape Factor</b>	<b>Test Loss (MSE)</b>	<b>% Change</b>	<b>Min. Test Error</b>	<b>Max. Test Error</b>
$C_D$	0.0724	-	$1.943 \times 10^{-4}$	0.7964
HEC-18	0.1580	+118%	$1.025 \times 10^{-4}$	1.5349
Neill	0.3424	+373%	$7.110 \times 10^{-7}$	4.8017
A&O	0.3503	+384%	$3.697 \times 10^{-4}$	5.1352

### 5.3.2 Inclusion of Flow Separation Velocity

Models were also optimized with different velocity scales including the flow separation velocity from the pier. The parameters selected to be tested were the same as those used in the field model analysis. The results of these results, compared to the original optimized model, are outlined in Table 5.9. The total error and maximum error values increased with the introduction of  $k$  (i.e.  $U_s/U$ ) in the scour prediction models. Conversely, the error values decreased when  $U_s/U_c$  was used as the velocity scale. This indicates that the critical bed material velocity has a significant impact on the scour predictions. The plot of predicted versus measured relative equilibrium scour depth for the  $U_s/U_c$  model can be found in Figure 5.9. Although a majority of the points have similar scour estimations as in the original model, an increase in error is evident in the higher  $d_{se}/D$  values, where the points lie closer to the exact-match line. The plot of predicted versus measured  $d_{se}/D$  for the model incorporating  $k$  as an input parameter can be found in Appendix B.

*Table 5.9: Comparison of combined ANNs with varying velocity scales*

<b>Velocity Scale</b>	<b>Test Error (MSE)</b>	<b>% Change</b>	<b>Min. Test Error</b>	<b>Max. Test Error</b>
$U/U_c$	0.0724	-	$1.943 \times 10^{-4}$	0.7964
$k$	0.1094	+51%	$2.237 \times 10^{-5}$	1.1378
$U_s/U_c$	0.0684	-6%	$8.907 \times 10^{-6}$	0.7484

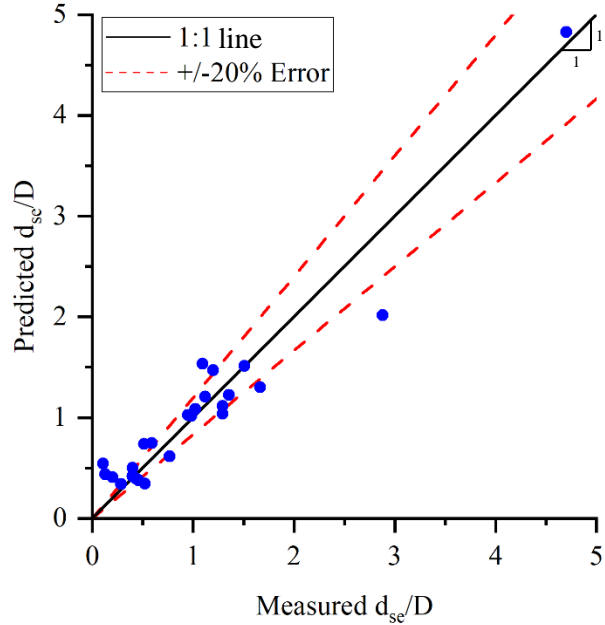


Figure 5.9: Predicted vs. actual  $d_{sc}/D$  for combination ANN with  $U_s/U_c$

The benefit of using the input parameter  $U_s/U_c$  over  $U/U_c$  or  $k$  is that it incorporates both of these parameters into one value. With the utilization of  $U_s/U_c$ , the approach flow velocity, blockage effects and critical bed material velocity are all taken into consideration. The inclusion of flow separation velocity from the bridge pier has a beneficial effect on the combined database, contrary to the field database, since blockage effects have a greater impact on laboratory data. This is due to the fact that the blockage ratio in laboratory experiments is typically higher than what is experienced in the field. Since the combined database contains data from both the field and laboratory conditions, blockage effects should be considered. The updated ANN, with  $U_s/U_c$  as the velocity scale instead of  $U/U_c$ , consists of two hidden layers with ten nodes within each layer and a learning rate of  $6.5 \times 10^{-3}$ .

### 5.3.3 Sensitivity Analysis

As with the laboratory-trained and field-trained models, the model trained on the combination database underwent a sensitivity analysis to validate the selection of input parameters and investigate their impact on the model. The results from the sensitivity analysis

are presented in Table 5.10. As can be observed from the table, each of the input parameters selected had valuable impact on the model, as the error increased significantly with the exclusion of each parameter. The largest increase of error was observed when  $\sigma_g$  was left out of the model, indicating that it has the greatest influence on the model. All other parameters, other than the relative coarseness of bed material, showed an increase in error between 100% and 200%, suggesting that the influence of these parameters is approximately the same. This includes the pier aspect ratio, further supporting the results from the field-trained network that L/D has an impact on the equilibrium scour depth even when the pier is in line with the approach flow. When D/d<sub>50</sub> was excluded from the model, the error experienced an increase of 78%, the lowest increase of all the inputs. This indicating that, although the relative coarseness of bed material adds significant value to the network, it is not as influential as the other parameters.

*Table 5.10: Sensitivity analysis results for combined-trained ANN*

<b>Missing Parameter</b>	<b>Test Loss (MSE)</b>	<b>% Change</b>	<b>Min. Test Error</b>	<b>Max. Test Error</b>
None	0.0684	-	$8.907 \times 10^{-6}$	0.7484
Fr	0.1682	+146%	$2.442 \times 10^{-6}$	2.6333
h/D	0.1477	+116%	$3.991 \times 10^{-4}$	1.1788
U <sub>s</sub> /U <sub>c</sub>	0.1531	+124%	$3.725 \times 10^{-4}$	1.5766
D/d <sub>50</sub>	0.1216	+78%	$5.468 \times 10^{-5}$	1.2037
L/D	0.1727	+152%	$2.689 \times 10^{-4}$	2.3161
C <sub>D</sub>	0.1904	+178%	$9.796 \times 10^{-5}$	1.1405
$\sigma_g$	0.8565	+1150%	$3.927 \times 10^{-4}$	16.718

### 5.3.4 Comparison to Other Prediction Models

Since the current ANN presented was proven to produce the most accurate scour depth estimations for field use out of the models developed, it is useful to compare the current model to empirical formulae as well as ANNs developed in literature. The ANNs that the current model is compared against are only those which were also developed for the purpose of field scour

estimates. Any models that were developed solely for the purpose of laboratory predictions were not considered.

#### 5.3.4.1 Prediction Equations

The combined ANN results were compared to those from empirical equations as was done for both the laboratory and field models. Table 5.11 outlines the error values from the combination-trained ANN and empirical formulae. Similar to what was observed for the first two ANNs developed, the predictions from the current model show significant improvement over any of the empirical equations. It is also observed that the correlation coefficient is very close to unity, indicating a strong linear relationship between the predicted and measured relative equilibrium scour depth values. The predicted versus measured  $d_{se}/D$  values were plotted for each of the empirical formulae and are presented in Figure 5.10.

As was observed with both the laboratory-trained and field-trained models, the combination-trained ANN produced relative equilibrium scour depth predictions with a higher degree of accuracy than each of the empirical formulae. This is evident since only a small percentage of the data falls within the 20% error bounds in each of the plots produced from the formulae. The Froelich (1988) equation severely underpredicted a majority of the scour depths, which could result in unsafe bridge foundation designs. Conversely, the HEC-18 (2001) and S/M (2011) equations both overestimated most of the scour depths. This overestimation results in bridge foundation designs that are not economical. Similar to the results with the field data, the S/M (2011) equation produced unrealistic negative  $d_{se}/D$  values. Negative scour depth estimations are harmful in bridge foundation design, as the design engineer has no indication of the scour that is expected to occur. The Williams (2016) equation both under and overestimated the relative equilibrium scour depths. However, this equation was developed mainly for laboratory

applications, therefore accurate field estimations were not anticipated. It is also important to note that none of the empirical equations were able to accurately predict the expected  $d_{sc}/D$  value for the outlier point (i.e., measured  $d_{sc}/D = 4.7$ ). In fact, this point was significantly underestimated with each of the equations. This suggests that the ANN is applicable to a larger range of scour data than the empirical equations.

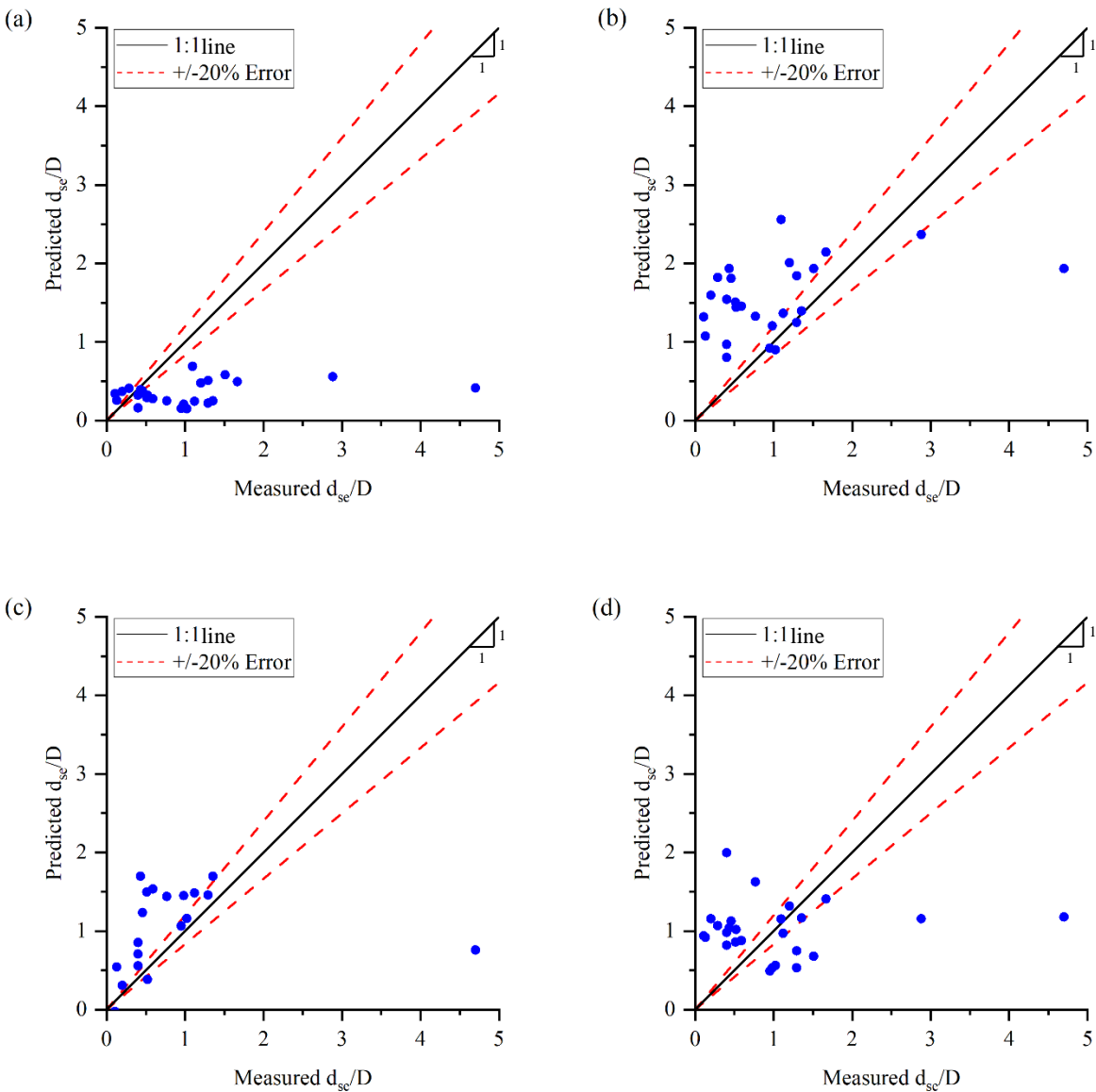


Figure 5.10: Predicted versus observed  $d_{sc}/D$  for the (a) Froelich (1988) equation, (b) HEC-18 equation, (c) S/M (2011) equation, and (d) Williams (2016) equation applied to combination data

Table 5.11: Comparison of error values from combined ANN against empirical formulae

<b>Error</b>	<b>ANN</b>	<b>Froelich (1988)</b>	<b>HEC-18 (2001)</b>	<b>S/M (2011)</b>	<b>Williams (2016)</b>
MSE	0.0684	1.2727	1.0389	3.4945	0.9849
MAE	0.1871	0.7181	0.8120	1.2241	0.7212
MAPE	44%	68%	204%	130%	149%
R	0.9618	0.3441	0.4221	-0.1661	0.0432

#### 5.3.4.2 ANNs in the Literature

The proposed ANN models were also compared to those found in the literature. Since the ANNs developed in the literature were not evaluated on the same test data as the current ANN, and the exact models are not available to apply the current test data set to, the comparisons to these models cannot be exact. To give a general comparison of how the models perform compared to one another, the error values reported in the literature are compared to those calculated in the current research. Many of the ANNs in the literature utilized the correlation coefficient and/or mean absolute percent error to evaluate the models' performance. The reported R and MAPE values from ANNs in the literature are presented in Table 5.12, along with the error values from the ANN developed in the current research.

Table 5.12: Comparison of present ANN to others found in literature

<b>ANN</b>	<b>R</b>	<b>MAPE</b>
Present Study (Combined-trained)	0.962	44%
Choi and Cheong (2006)	-	65%
Lee et al. (2007)	0.956	-
Kaya (2010)	0.926	59%
Toth and Brandimarte (2011)	-	58%
Bonakdari and Ebtehaj (2017)	-	69%
Pal (2019)	0.962	-
Shamshirband et al. (2020)	0.880	-

As can be seen from the table, the current ANN has the most favourable R and MAPE values compared to those found in the literature. An exception to this is the model proposed by Pal (2019), where the R value is equal to that calculated from the current model. However, the model proposed by Pal (2019) is considerably more computationally expensive, with 10,000 epochs, 3

hidden layers consisting of 100, 80, and 50 nodes, and dropout layers, allowing the model to produce results similar in accuracy to the current model. The structure and computational requirements of the ANN from the current study is significantly simpler. The current ANN utilizes physics-based parameters to allow the model to train on the data with less computational expense. The model proposed by Lee et al. (2007) also produces an R value that is relatively close to that produced by the current model. However, similar to the case with Pal (2019), the computational costs are significantly greater. Although the structure of the model presented by Lee et al. (2007) is simpler than the current model, with one hidden layer and six nodes within that layer, the model requires 10,000 epochs to train. Both the models presented by Pal (2019) and Lee et al. (2007) were able to produce scour estimates with similar accuracy as the current proposed model, however they require 50 times the number of epochs to produce these results.

#### **5.4 Scour Width Model**

The final model developed was the scour width prediction model, which was created to predict both equilibrium scour depth and width. Due to the lack of scour width data available for field measurements, a scour width model was trained exclusively on laboratory data. As a result, the model developed would be applicable to laboratory conditions only, while the implementation of the model for field conditions is unknown. However, development of a scour width model with the use of laboratory data allows for evaluation of the feasibility of a model developed with field data.

The input parameters selected for the model were the same as the set used to develop the laboratory-trained model, as presented in equation (5.1). The optimized network consisted of one hidden layer with six nodes within that layer and a learning rate of  $1.1 \times 10^{-3}$ . It was found that the model performance was optimized with the inputs being scaled on a range of zero to one and

with the use of the sigmoid activation function. The predicted versus measured relative equilibrium scour width and depth values are plotted in Figure 5.11. From this figure, it is evident that the model is able to produce both accurate scour depth and width values, with only a few data points falling outside of the 20% error bounds. Additionally, a majority of the scour width points, along with a significant amount of the scour depth points lie in close proximity to the exact-match line.

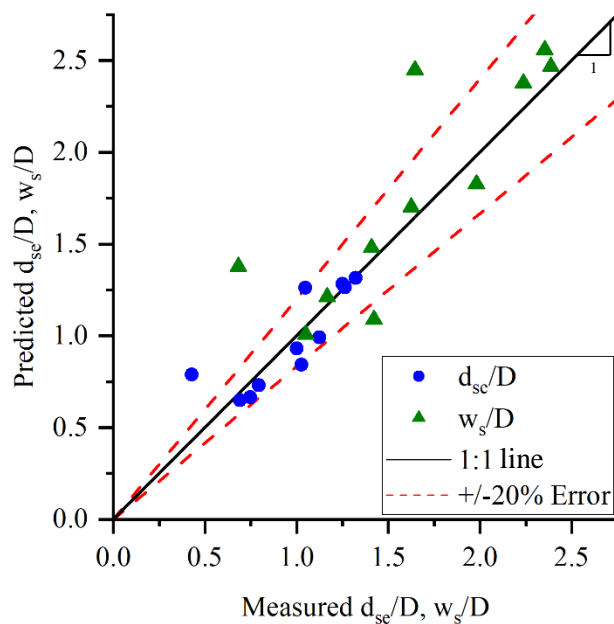


Figure 5.11: Predicted vs. measured  $d_{sc}/D$  and  $w_s/D$  for scour width model

#### 5.4.1 Inclusion of Blockage Effects

As was done with the laboratory-trained model, the optimization process was repeated excluding the blockage ratio to analyse its effects on the scour width predictions. The results from the model without  $D/B$  compared to the model including  $D/B$  are presented in Table 5.13. It is observed that the total loss increases by 109%, indicating that, like the scour depth, the blockage ratio also has significant influence on the scour width. The maximum test error also increases significantly with the exclusion of  $D/B$ , further re-iterating the importance of blockage

effects on scour development in laboratory conditions. The plot of predicted versus measured scour values for the model without D/B is found in Appendix B.

*Table 5.13: Results of blockage effects investigation on scour width model*

<b>Model</b>	<b>Test Loss (MSE)</b>	<b>% Change</b>	<b>Min. Test Error</b>	<b>Max. Test Error</b>
With D/B	0.0726	-	$1.724 \times 10^{-3}$	0.3458
Re-optimized No D/B	0.1519	+109%	$5.755 \times 10^{-4}$	1.1466

#### 5.4.1.1 Flow Separation Velocity

Since the blockage effects can also be integrated into the model with the flow separation velocity from the pier, ANNs were also optimized with input parameters incorporating  $U_s$ , to evaluate their applicability to the scour width prediction model. The results of the models including  $U_s$ , compared to the results of the original model, can be found in Table 5.14. Since the scour width model is based on laboratory data, the densimetric Froude number, calculated with  $U_s$ , (equation (2.7a)) was also considered. This value was not considered for field data, as the specific gravity of the bed material is required, and this value is rarely reported for field data. It is observed that the total error as well as the maximum error increase with the inclusion of  $k$  as an input parameter. Conversely, both of these error values are decreased when  $U_s/U_c$  is considered as an input. For the model including  $F_{ds}$  as an input parameter, the total error increased slightly, while the maximum test error decreased.

*Table 5.14: Comparison of scour width ANNs with varying velocity scales*

<b>Velocity Scale</b>	<b>Test Loss (MSE)</b>	<b>% Change</b>	<b>Min. Test Error</b>	<b>Max. Test Error</b>
$U/U_c$	0.0726	-	$1.724 \times 10^{-3}$	0.3458
$k$	0.1279	+76%	$4.718 \times 10^{-4}$	0.5922
$U_s/U_c$	0.0472	-35%	$9.599 \times 10^{-4}$	0.1565
$F_{ds}$	0.0793	+9%	$2.450 \times 10^{-3}$	0.2640

To further evaluate the applicability of the  $U_s/U_c$  parameter, the plot of predicted versus measured relative scour values is presented in Figure 5.12. From this figure it is evident that,

although the error values are decreased, the quality of the scour estimations have decreased. In Figure 5.12 there is a lower percentage of data points lying in close proximity to the exact-match line than what was observed in Figure 5.11. However, the values that were heavily overpredicted in the original model now fall closer to the 20% error bounds, while still not falling within them. The increase in accuracy of these values is likely what causes the overall test error value to decrease. After evaluating the predicted versus measured scour value plots, the original model was selected for further analysis, as the model was more accurate for a larger percentage of the test data set. The plot of predicted versus measured  $w_s/D$  and  $d_{sc}/D$  values for the models with  $k$  and  $F_{ds}$  as input parameters can be found in Appendix B.

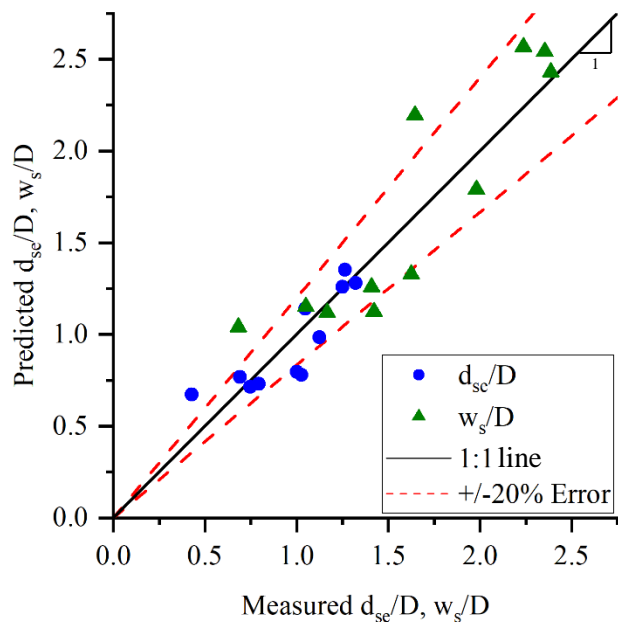


Figure 5.12: Predicted vs. actual  $d_{sc}/D$  and  $w_s/D$  for scour width ANN with  $U_s/U_c$

### 5.4.2 Sensitivity Analysis

A sensitivity analysis was conducted to validate the selection of input parameters and evaluate their influence on the scour prediction model. Table 5.15 outlines the results from this analysis. It is observed that all error values decreased when the Froude number was excluded from the model. This indicates that the inclusion of the Froude number as an input parameter did

not add significant value to the prediction model. The Froude number may not have had a meaningful influence on the scour width estimations as the scour database used in the training of the model only consisted of data from seven separate laboratory investigations. Additionally, in many of these investigations, the Froude number was held constant throughout each experiment conducted. As a result, there is not a significant amount of variation of Froude number in the scour width database. To further investigate the effect of Fr on the model, the  $d_{se}/D$  and  $w_s/D$  estimates were evaluated separately. In this investigation, it was found that although the scour width estimations improved with the removal of Fr, the scour depth estimations reduced in accuracy. The results of the sensitivity analysis also suggest that the scour prediction model heavily weighs the influence of flow intensity, with an error increase of 100%, while the exclusion of all other parameters resulted in an increase of less than 10%. This indicates that although the  $D/B$ ,  $h/D$  and  $D/d_{50}$  parameters add value to the prediction model, their impact is not significant compared to that of  $U/U_c$ . Subsequent analysis of the ANN was conducted without the inclusion of the Froude number as an input parameter, as this model produced the most accurate scour estimations.

*Table 5.15: Sensitivity analysis results for scour width ANN*

<b>Missing Parameter</b>	<b>Test Loss (MSE)</b>	<b>% Change</b>	<b>Min. Test Error</b>	<b>Max. Test Error</b>
None	0.0726	-	$1.724 \times 10^{-3}$	0.3458
Fr	0.0619	-15%	$3.538 \times 10^{-4}$	0.2936
D/B	0.0754	+4%	$9.808 \times 10^{-4}$	0.3582
h/D	0.0788	+9%	$3.079 \times 10^{-3}$	0.3905
$U/U_c$	0.1452	+100%	$1.267 \times 10^{-3}$	0.8047
$D/d_{50}$	0.0737	+2%	$1.670 \times 10^{-3}$	0.3346

### 5.4.3 Comparison to Prediction Equation

Since the model predicts both scour depth and scour width values, the model was compared to two different sets of equations. First, the scour width predictions from the model were

compared to those from the HEC-18 scour width equation. As discussed in Section 2.3.2., there is a significant difference in the performance of the HEC-18 scour width prediction equation if the  $d_{se}$  value is known versus unknown. For the sake of comparison, the  $w_s$  equation was applied to both situations. However, in practice, when designing bridge foundations, the scenario in which the  $d_{se}$  value is not known would be the only case which would occur. Various error values calculated from the scour width predictions are presented in Table 5.16. From the table it is evident that the scour width predictions from the ANN are significantly more accurate than the estimations made with the equation. The improvement from the predictions as a result of applying the equation with  $d_{se}$  unknown to the predictions from the ANN is especially substantial. For further analysis, plots of predicted versus measured  $w_s/D$  values are presented in Figure 5.13. When comparing this plot to Figure 5.11, it is evident that the ANN is able to predict  $w_s/D$  values with more accuracy than the HEC-18 equation when the  $d_{se}$  is either known or unknown. For the case in which the  $d_{se}$  values are not known, none of the predictions fall within the 20% error bound and the predictions are considerably overestimated. These high estimates of expected scour width values can negatively effect bridge foundation design, especially when piers are in close proximity to one another.

*Table 5.16: Comparison of error values from scour width model to HEC-18 (2001) scour width equation*

<b>Error</b>	<b>ANN</b>	<b>Equation – <math>d_{se}</math> known</b>	<b>Equation – <math>d_{se}</math> unknown</b>
MSE	0.0988	0.3148	2.8159
MAE	0.1942	0.4097	1.5579
MAPE	18%	44%	147%
R	0.8624	0.7858	0.3724

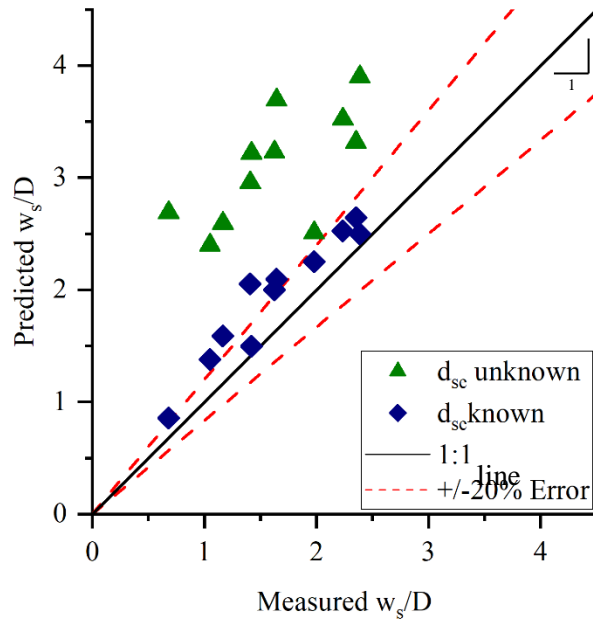


Figure 5.13: Predicted vs. observed  $w_s/D$  for HEC-18 (2001) scour width equation, with  $d_{sc}/D$  values known and unknown

Table 5.17 outlines the comparison of the ANN relative equilibrium scour depth estimations to those from empirical formulae. It is observed that, similar to the scour width predictions, the ANN produces the most favourable error values for each of the errors calculated. This indicates that the model is able to produce more accurate relative equilibrium scour depth measurements than the equations proposed in the literature. Plots of predicted versus measured  $d_{sc}/D$  values were also created and are presented in Figure 5.14. These plots further re-iterate the results that have been observed among all other models compared to the empirical equations. Once again, the present model was able to produce the most accurate  $d_{sc}/D$  predictions when compared to empirical equations. Results from the current model indicate that it is feasible to develop an ANN that is able to predict both equilibrium scour width and equilibrium scour depth values for use in foundation design practice if the data required becomes available.

Table 5.17: Comparison of error values from scour width model to various empirical  $d_{sc}/D$  equations

Error	ANN	Froelich (1988)	HEC-18 (2001)	S/M (2011)	Williams (2016)
MSE	0.0250	0.2627	0.3253	0.4261	0.4621
MAE	0.1367	0.4474	0.5197	0.5990	0.6142
MAPE	18%	61%	65%	63%	62%
R	0.8223	0.7254	0.7006	0.8539	-0.5224

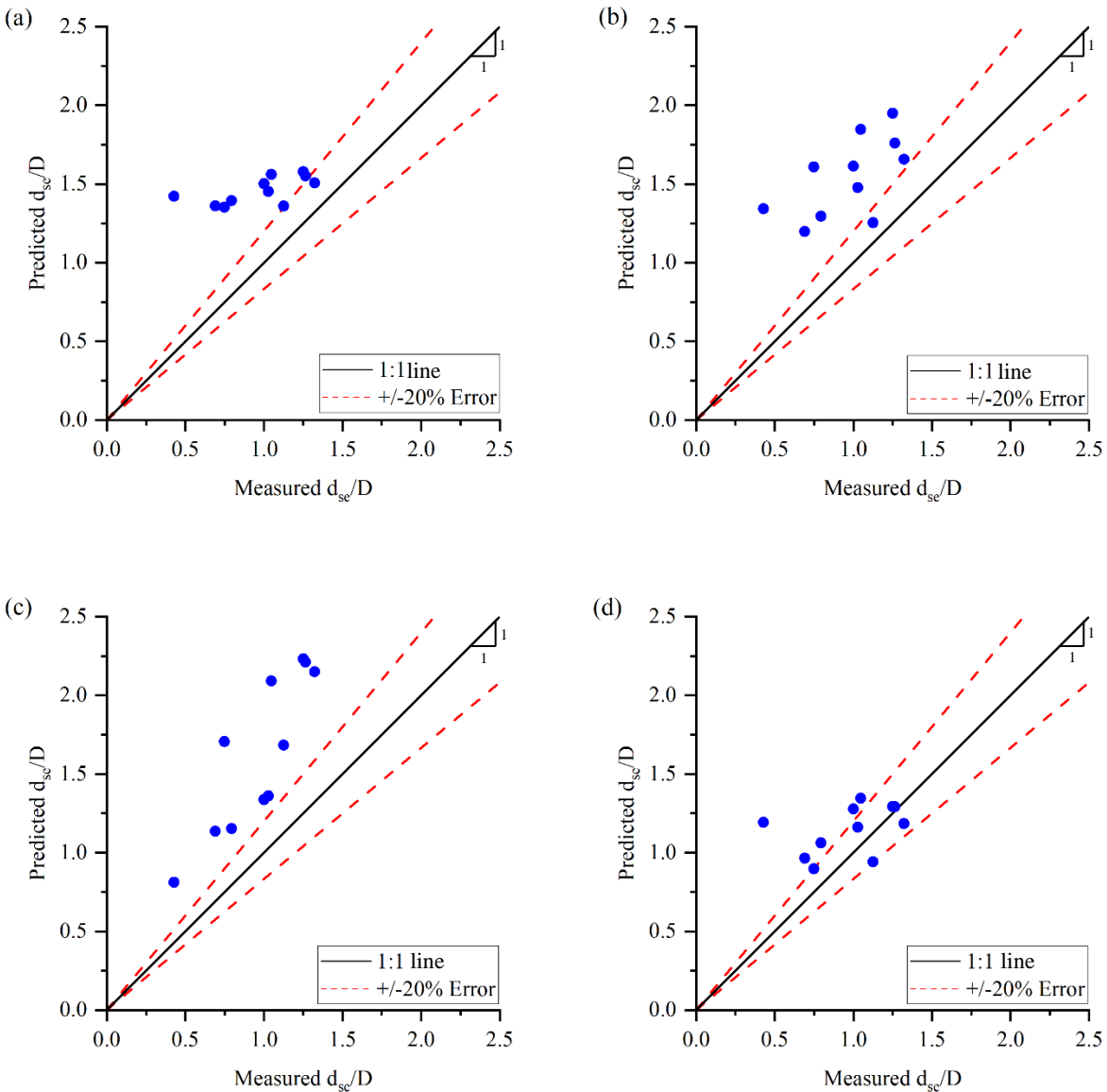


Figure 5.14: Predicted versus observed  $d_{sc}/D$  for the (a) Froelich (1988) equation, (b) HEC-18 equation, (c) S/M (2011) equation, and (d) Williams (2016) equation applied to depth data within scour width database

## CHAPTER 6

### CONCLUSIONS

#### 6.1 Summary

Accurate scour depth and width ( $d_{se}/D$  and  $w_s/D$ ) estimations are crucial for safe and economical bridge foundation designs. Current design practice employs the use of empirical formulae, typically developed by curve-fitting to laboratory data. These equations tend to be limited to certain geometric and flow conditions and extrapolating to field situations should be done with caution. Recently, investigations into the applications of artificial neural networks (ANNs) to the pier scour problem have been conducted. ANN can be used to mitigate some of the major shortcomings that arise through curve-fitting. These investigations have resulted in improved accuracy of scour depth estimations for both laboratory and field use. However, the laboratory ANN estimations have a significantly higher degree of accuracy than those in field conditions.

The current investigation involved exploring the use of physics-aware parameters and a combination of laboratory and field data in an attempt to improve field scour estimations with ANNs. The applicability of ANNs for scour width predictions was also investigated. A total of four final neural networks were developed and compared to empirical formulae. A summary of the networks is presented in Table 6.1, with the combination network being optimal for field scour prediction.

Table 6.1: Summary of ANNs developed

ANN	No. of hidden layers	No. of hidden nodes	Learning rate	No. of Epochs	Input scaling method	Activation function
Laboratory	3	5	$2.0 \times 10^{-2}$	150	[0,1]	Sigmoid
Field	1	13	$3.3 \times 10^{-3}$	200	$\bar{X}_N=0, \sigma_N=1$	Sigmoid
Combination	1	11	$6.7 \times 10^{-3}$	200	[0,1]	Sigmoid
Width	1	6	$1.1 \times 10^{-3}$	150	[0,1]	Sigmoid

From this investigation, the following conclusions can be drawn:

- When applied to field conditions, laboratory-trained models are unable to produce scour depth estimations with the same level of accuracy as in the laboratory predictions.
- The accuracy of field scour depth estimations increases when the model is trained on a data set composed of mainly field data with some laboratory data to support the training process.
- Introducing  $C_D$ , a physics-based parameter, to a network to incorporate pier shape as opposed to empirical shape factors results in more accurate  $d_{se}/D$  predictions.
- For models trained on laboratory data, the error produced from  $d_{se}/D$  estimates is decreased by including  $U_s$  as a physics-based parameter to incorporate blockage effects in the model.
- The agreement of  $d_{se}/D$  and  $w_s/D$  predictions from the scour width ANN with measured values indicate the viability of a single ANN for both  $d_{se}/D$  and  $w_s/D$  predictions.
- All the ANNs developed produced significantly more accurate scour estimations and were applicable to a larger range of data than the presently used empirical equations.

## 6.2 Recommendations

Recommendations for future studies include the investigation of restraining underprediction for ANN scour estimates. Although ANNs are able to produce more accurate scour predictions than empirical formulae, the models cannot distinguish between under and overestimations. The ability to ensure no predictions are underestimated would be a valuable asset to a scour prediction model. It is also recommended that more diverse laboratory data (e.g., varying pier shapes and pier aspect ratios) be collected to support the training of the combined model. An increase in accuracy of the combined model may result from more diverse data, as laboratory data used to support the training of the ANN was restricted to circular cylinders alone. Providing a wider range of supporting data may aid the model in predicting scour at varying piers for field applications. Finally, the collection of scour width data, for the purpose of model training is recommended. As observed from the scour depth model, ANNs trained solely on laboratory data do not necessarily translate well to field use. The collection of sufficient scour width data from the field would allow for the development of a scour width ANN to be used in practice for foundation design.

## REFERENCES

- Ahmed, F., & Rajaratnam, N. (1998). Flow around Bridge Piers. *Journal of Hydraulic Engineering*, 124(3), 288–300. [https://doi.org/10.1061/\(ASCE\)0733-9429\(1998\)124:3\(288\)](https://doi.org/10.1061/(ASCE)0733-9429(1998)124:3(288))
- Akiba, T., Sano, S., Yanase, T., Ohta, T., & Koyama, M. (2019). Optuna: A Next-generation Hyperparameter Optimization Framework. *Proceedings of the 25th ACM SIGKDD International Conference on Knowledge Discovery & Data Mining*, 2623–2631. <https://doi.org/10.1145/3292500.3330701>
- Aksoy, A., & Eski, O. (2016). Experimental Investigation of Local Scour around Circular Bridge Piers Under Steady State Flow Conditions. *Journal of the South African Institution of Civil Engineering*, 58(3), 21–27. <https://doi.org/10.17159/2309-8775/2016/v58n3a3>
- Aksoy, A. O., Bombar, G., Arkis, T., & Guney, M. S. (2017). Study of the Time-dependent Clear Water Scour around Circular Bridge Piers. *Journal of Hydrology and Hydromechanics*, 65(1), 26–34. <https://doi.org/10.1515/johh-2016-0048>
- Al-Shukur, A., & Obeid, Z. H. (2016). Experimental Study of Bridge Pier Shape to Minimize Local Scour. *International Journal of Civil Engineering and Technology*, 7(1), 162–171.
- Amini, A., Hamidi, S., Shirzadi, A., Behmanesh, J., & Akib, S. (2020). Efficiency of Artificial Neural Networks in Determining Scour Depth at Composite Bridge Piers. *International Journal of River Basin Management*, 19(3), 327–333. <https://doi.org/10.1080/15715124.2020.1742138>
- Batani, S. M., Borghei, S. M., & Jeng, D.-S. (2007). Neural network and neuro-fuzzy assessments for scour depth around bridge piers. *Engineering Applications of Artificial Intelligence*, 20(3), 401–414. <https://doi.org/10.1016/j.engappai.2006.06.012>
- Benedict, S. T., & Caldwell, A. W. (2014). *A Pier-Scour Database: 2,427 Field and Laboratory Measurements of Pier Scour Data* (Data Series) [Data Series]. United States Geological Survey.
- Bonakdari, H., & Ebtehaj, I. (2017). Scour Depth Prediction around Bridge Piers Using Neuro-Fuzzy and Neural Network Approaches. *International Journal of Civil and Environmental Engineering*, 11(6), 835–839.
- Braich, B., & Mendoza, G. P. (2022, February 5). The race to repair B.C.'s Coquihalla Highway. *CBC News*. <https://www.cbc.ca/newsinteractives/features/coquihalla-repaired-35-days>
- Breusers, H. N. C., Nicollet, G., & Shen, H. W. (1977). Local Scour Around Cylindrical Piers. *Journal of Hydraulic Research*, 15(3), 211–252. <https://doi.org/10.1080/00221687709499645>
- Chabert, J., & Engeldinger, P. (1956). *Etude des affouillements autour des piles de ponts*. Laboratoire National d'Hydraulique.
- Chiew, Y.-M. (1984). *Local Scour at Bridge Piers*. [Doctoral dissertation, The University of Auckland, New Zealand]. University of Auckland Research Repository – ResearchSpace.

- Choi, S.-U., & Cheong, S. (2006). Prediction of Local Scour around Bridge Piers using Artificial Neural Networks. *Journal of the American Water Resources Association*, 42(2), 487–494. <https://doi.org/10.1111/j.1752-1688.2006.tb03852.x>
- Cook, W. (2014). *Bridge Failure Rates, Consequences, and Predictive Trends*. [Doctoral dissertation, Utah State University]. Utah State University Digital Commons. <https://doi.org/10.26076/bfec-580b>
- Coscarella, F., Gaudio, R., & Manes, C. (2020). Near-bed Eddy Scales and Clear-water Local Scouring around Vertical Cylinders. *Journal of Hydraulic Research*, 58(6), 968–981. <https://doi.org/10.1080/00221686.2019.1698668>
- D'Alessandro, C. (2013). *Effect of Blockage on Cylindrical Bridge Pier Local Scour*. [MAsc thesis, University of Windsor]. Scholarship at UWindsor. <https://scholar.uwindsor.ca/etd/4966>
- Deng, L., & Cai, C. S. (2010). Bridge Scour: Prediction, Modeling, Monitoring, and Countermeasures—Review. *Practice Periodical on Structural Design and Construction*, 15(2), 125–134. [https://doi.org/10.1061/\(ASCE\)SC.1943-5576.0000041](https://doi.org/10.1061/(ASCE)SC.1943-5576.0000041)
- Dey, S., Bose, S. K., & Sastry, G. L. N. (1995). Clear Water Scour at Circular Piers: A Model. *Journal of Hydraulic Engineering*, 121(12), 869–876. [https://doi.org/10.1061/\(ASCE\)0733-9429\(1995\)121:12\(869\)](https://doi.org/10.1061/(ASCE)0733-9429(1995)121:12(869))
- Ettema, R. (1980). *Scour at Bridge Piers* (No. 216). Department of Civil Engineering, University of Auckland.
- Ettema, R., Constantinescu, G., & Melville, B. W. (2011). *NCHRP Web-Only Document 175: Evaluation of Bridge Scour Research: Pier Scour Processes and Predictions*. Washington, DC: Research Board of National Academies. <https://doi.org/10.17226/22886>
- Ettema, R., Kirkil, G., & Muste, M. (2006). Similitude of Large-Scale Turbulence in Experiments on Local Scour at Cylinders. *Journal of Hydraulic Engineering*, 132(1), 33–40. [https://doi.org/10.1061/\(ASCE\)0733-9429\(2006\)132:1\(33\)](https://doi.org/10.1061/(ASCE)0733-9429(2006)132:1(33))
- Ettema, R., Melville, B. W., & Barkdoll, B. (1998). Scale Effect in Pier-Scour Experiments. *Journal of Hydraulic Engineering*, 124, 639–642.
- Falcon, W., Borovec, J., Wälchli, A., Eggert, N., Schock, J., Jordan, J., Skafte, N., Ir1dXD, Bereznyuk, V., Harris, E., Murrell, T., Yu, P., Præsius, S., Addair, T., Zhong, J., Lipin, D., Uchida, S., Bapat, S., Schröter, H., ... Bakhtin, A. (2020). *PyTorchLightning/pytorch-lightning: 0.7.6 release*. Zenodo. <https://doi.org/10.5281/zenodo.3828935>
- Froehlich, D. C. (1988). Analysis of onsite measurements of scour at piers. *Proceedings of the 1988 ASCE National Hydraulic Engineering Conference*, 534–539. <https://pubs.er.usgs.gov/publication/70014448>
- Garg, R. K., Chandra, S., & Kumar, A. (2022). Analysis of Bridge Failures in India from 1977 to 2017. *Structure and Infrastructure Engineering*, 18(3), 295–312. <https://doi.org/10.1080/15732479.2020.1832539>

- Guo, J. (2012). Pier Scour in Clear Water for Sediment Mixtures. *Journal of Hydraulic Research*, 50(1), 18–27. <https://doi.org/10.1080/00221686.2011.644418>
- Hodi, B. (2009). *Effect of Blockage and Densimetric Froude Number on Circular Bridge Pier Local Scour*. [MASC thesis, University of Windsor]. Scholarship at UWindsor. <https://scholar.uwindsor.ca/etd/79>
- Hunter, J. D. (2007). Matplotlib: A 2D Graphics Environment. *Computing in Science & Engineering*, 9(3), 90–95. <https://doi.org/10.1109/MCSE.2007.55>
- Johnson, A., & Torrico, E. F. (1995). Scour Around Wide Piers in Shallow Water. *Transportation Research Record*, 1417, 66–70.
- Kaya, A. (2010). Artificial Neural Network Study of Observed Pattern of Scour Depth around Bridge Piers. *Computers and Geotechnics*, 37(3), 413–418. <https://doi.org/10.1016/j.compgeo.2009.10.003>
- Khaple, S., Hanmaiahgari, P. R., Gaudio, R., & Dey, S. (2017). Interference of an upstream pier on local scour at downstream piers. *Acta Geophysica*, 65(1), 29–46. <https://doi.org/10.1007/s11600-017-0004-2>
- Kharbeche, M. (2022). *The Role of Pier Shape and Aspect Ratio on Local Scour with and without Sacrificial Piles*. [MASC thesis, University of Windsor]. Scholarship at UWindsor. <https://scholar.uwindsor.ca/etd/8791>
- Khwairakpam, P., Ray, S. S., Das, S., Das, R., & Mazumdar, A. (2012). Scour Hole Characteristics around a Vertical Pier under Clearwater Scour Conditions. *ARPJ Journal of Engineering and Applied Sciences*, 7(6), 649–654.
- Kingma, D. P., & Ba, J. (2017). *Adam: A Method for Stochastic Optimization* (arXiv:1412.6980). arXiv. <http://arxiv.org/abs/1412.6980>
- Kothyari, U. C., & Kumar, A. (2012). Temporal Variation of Scour around Circular Compound Piers. *Journal of Hydraulic Engineering*, 138(11), 945–957. [https://doi.org/10.1061/\(ASCE\)HY.1943-7900.0000593](https://doi.org/10.1061/(ASCE)HY.1943-7900.0000593)
- Lanca, R. M., Fael, C. S., Maia, R. J., Pego, J. P., & Cardoso, A. H. (2013). Clear-Water Scour at Comparatively Large Cylindrical Piers. *Journal of Hydraulic Engineering*, 139(11), 1117–1125. [https://doi.org/10.1061/\(ASCE\)HY.1943-7900.0000788](https://doi.org/10.1061/(ASCE)HY.1943-7900.0000788)
- Laursen, E. M., & Toch, A. (1956). Scour Around Bridge Piers And Abutments. *Iowa Highway Research Board*, 4.
- Lee, S. O., & Sturm, T. W. (2009). Effect of Sediment Size Scaling on Physical Modeling of Bridge Pier Scour. *Journal of Hydraulic Engineering*, 135(10), 793–802. [https://doi.org/10.1061/\(ASCE\)HY.1943-7900.0000091](https://doi.org/10.1061/(ASCE)HY.1943-7900.0000091)
- Lee, T. L., Jeng, D. S., Zhang, G. H., & Hong, J. H. (2007). Neural Network Modeling for Estimation of Scour Depth Around Bridge Piers. *Journal of Hydrodynamics*, 19(3), 378–386. [https://doi.org/10.1016/S1001-6058\(07\)60073-0](https://doi.org/10.1016/S1001-6058(07)60073-0)

- Link, O., Henríquez, S., & Ettmer, B. (2019). Physical Scale Modelling of Scour around Bridge Piers. *Journal of Hydraulic Research*, 57(2), 227–237. <https://doi.org/10.1080/00221686.2018.1475428>
- Manes, C., & Brocchini, M. (2015). Local Scour around Structures and the Phenomenology of Turbulence. *Journal of Fluid Mechanics*, 779, 309–324. <https://doi.org/10.1017/jfm.2015.389>
- Melville, B. W. (1997). Pier and Abutment Scour: Integrated Approach. *Journal of Hydraulic Engineering*, 123(2), 125–136. [https://doi.org/10.1061/\(ASCE\)0733-9429\(1997\)123:2\(125\)](https://doi.org/10.1061/(ASCE)0733-9429(1997)123:2(125))
- Melville, B. W., & Chiew, Y.-M. (1999). Time Scale for Local Scour at Bridge Piers. *Journal of Hydraulic Engineering*, 125(1), 59–65. [https://doi.org/10.1061/\(ASCE\)0733-9429\(1999\)125:1\(59\)](https://doi.org/10.1061/(ASCE)0733-9429(1999)125:1(59))
- Melville, B. W., & Sutherland, A. J. (1988). Design Method for Local Scour at Bridge Piers. *Journal of Hydraulic Engineering*, 114(10), 1210–1226. [https://doi.org/10.1061/\(ASCE\)0733-9429\(1988\)114:10\(1210\)](https://doi.org/10.1061/(ASCE)0733-9429(1988)114:10(1210))
- Mia, Md. F., & Nago, H. (2003). Design Method of Time-Dependent Local Scour at Circular Bridge Pier. *Journal of Hydraulic Engineering*, 129(6), 420–427. [https://doi.org/10.1061/\(ASCE\)0733-9429\(2003\)129:6\(420\)](https://doi.org/10.1061/(ASCE)0733-9429(2003)129:6(420))
- Miroff, N. (2007, August 3). Collapse Spotlights Weaknesses in U.S. Infrastructure. *Washington Post*, [www.washingtonpost.com](http://www.washingtonpost.com)
- Neill, C.R. (1973). Guide to Bridge Hydraulics. *Road and Transportation Association of Canada*, University of Toronto, Toronto, Ont.
- Norberg, C. (1987). *Effects of Reynolds Number and a Low-Intensity Freestream Turbulence on the Flow around a Circular Cylinder* (Nr. 87/2). Chalmers University of Technology, Gothenburg, Sweden.
- Pal, M. (2019). Deep neural network based pier scour modeling. *ISH Journal of Hydraulic Engineering*, 28(sup1), 80–85. <https://doi.org/10.1080/09715010.2019.1679673>
- Pandey, M., Azamathulla, H. M., Chaudhuri, S., Pu, J. H., & Pourshahbaz, H. (2020a). Reduction of time-dependent scour around piers using collars. *Ocean Engineering*, 213, 1-15. <https://doi.org/10.1016/j.oceaneng.2020.107692>
- Pandey, M., Sharma, P. K., Ahmad, Z., & Singh, U. K. (2017). Evaluation of Existing Equations for Temporal Scour Depth around Circular Bridge Piers. *Environmental Fluid Mechanics*, 17(5), 981–995. <https://doi.org/10.1007/s10652-017-9529-9>
- Pandey, M., Zakwan, M., Khan, M. A., & Bhave, S. (2020b). Development of scour around a circular pier and its modelling using genetic algorithm. *Water Supply*, 20(8), 3358–3367. <https://doi.org/10.2166/ws.2020.244>
- Paszke, A., Gross, S., Massa, F., Lerer, A., Bradbury, J., Chanan, G., Killeen, T., Lin, Z., Gimelshein, N., Antiga, L., Desmaison, A., Kopf, A., Yang, E., DeVito, Z., Raison, M., Tejani, A., Chilamkurthy, S., Steiner, B., Fang, L., ... Chintala, S. (2019). PyTorch: An Imperative Style,

- High-Performance Deep Learning Library. *Advances in Neural Information Processing Systems*, 32. <https://papers.nips.cc/paper/2019/hash/bdbca288fee7f92f2bfa9f7012727740-Abstract.html>
- Raikar, R. V., & Dey, S. (2005). Clear-water Scour at Bridge Piers in Fine and Medium Gravel Beds. *Canadian Journal of Civil Engineering*, 32(4), 775–781. <https://doi.org/10.1139/105-022>
- Ramamurthy, A. S., & Lee, P. M. (1973). Wall Effects on Flow Past Bodies. *Journal of Sound and Vibration*, 31(4), 443–451. [https://doi.org/10.1016/S0022-460X\(73\)80259-7](https://doi.org/10.1016/S0022-460X(73)80259-7)
- Raudkivi, A. J., & Ettema, R. (1983). Clear-Water Scour at Cylindrical Piers. *Journal of Hydraulic Engineering*, 109(3), 338–350. [https://doi.org/10.1061/\(ASCE\)0733-9429\(1983\)109:3\(338\)](https://doi.org/10.1061/(ASCE)0733-9429(1983)109:3(338))
- Richardson, E.V. & Abed, L. (1993). Topwidth of Pier Scour Holes in Free and Pressure Flow. *ASCE Hydraulic Engineering, Proc. 1993 National Conference*, San Francisco, California.
- Richardson, E., & Davis, S. (2001). *Evaluating Scour at Bridges* (Fifth Edition). Federal Highway Administration, Washington, D.C.
- Roshko, A. (1955). *Some Measurements of Flow in a Rectangular Cutout*. National Advisory Committee for Aeronautics, Washington, DC. <https://resolver.caltech.edu/CaltechAUTHORS:20141114-111545203>
- Roshko, A. (1961). Experiments on the Flow Past a Circular Cylinder at Very High Reynolds Number. *Journal of Fluid Mechanics*, 10(3), 345–356. <https://doi.org/10.1017/S0022112061000950>
- Shamshirband, S., Mosavi, A., & Rabczuk, T. (2020). Particle Swarm Optimization Model to Predict Scour Depth around a Bridge Pier. *Frontiers of Structural and Civil Engineering*, 14(4), 855–866. <https://doi.org/10.1007/s11709-020-0619-2>
- Sheppard, D. M., Demir, H., & Melville, B. W. (2011). *NCHRP Report 682: Scour at Wide Piers and Long Skewed Piers*. Transportation Research Board, Washington, D.C.
- Sheppard, D. M., & Miller, W. (2006). Live-Bed Local Pier Scour Experiments. *Journal of Hydraulic Engineering*, 132(7), 635–642. [https://doi.org/10.1061/\(ASCE\)0733-9429\(2006\)132:7\(635\)](https://doi.org/10.1061/(ASCE)0733-9429(2006)132:7(635))
- Sheppard, D. M., Odeh, M., & Glasser, T. (2004). Large Scale Clear-Water Local Pier Scour Experiments. *Journal of Hydraulic Engineering*, 130(10), 957–963. [https://doi.org/10.1061/\(ASCE\)0733-9429\(2004\)130:10\(957\)](https://doi.org/10.1061/(ASCE)0733-9429(2004)130:10(957))
- Sheppard, D., Melville, B., & Demir, H. (2014). Evaluation of Existing Equations for Local Scour at Bridge Piers. *Journal of Hydraulic Engineering*, 140, 14–23. [https://doi.org/10.1061/\(ASCE\)HY.1943-7900.0000800](https://doi.org/10.1061/(ASCE)HY.1943-7900.0000800)
- Shirole, A. M., & Holt, R. C. (1991). Planning for a Comprehensive Bridge Safety Assurance Program. *Transportation Research Record*, 1290. <https://trid.trb.org/view/358683>
- Simarro, G., Fael, C. M. S., & Cardoso, A. H. (2011). Estimating Equilibrium Scour Depth at Cylindrical Piers in Experimental Studies. *Journal of Hydraulic Engineering*, 137(9), 1089–1093. [https://doi.org/10.1061/\(ASCE\)HY.1943-7900.0000410](https://doi.org/10.1061/(ASCE)HY.1943-7900.0000410)

- Tejada, S. (2014). *Effects of Blockage and Relative Coarseness on Clear Water Bridge Pier Scour*. [MAsc thesis, University of Windsor]. Scholarship at UWindsor. <https://scholar.uwindsor.ca/etd/5055>
- Ting, F. C. K., Briaud, J.-L., Chen, H. C., Gudavalli, R., Perugu, S., & Wei, G. (2001). Flume Tests for Scour in Clay at Circular Piers. *Journal of Hydraulic Engineering*, 127(11), 969–978. [https://doi.org/10.1061/\(ASCE\)0733-9429\(2001\)127:11\(969\)](https://doi.org/10.1061/(ASCE)0733-9429(2001)127:11(969))
- Toth, E., & Brandimarte, L. (2011). Prediction of Local Scour Depth at Bridge Piers Under Clear-water and Live-bed Conditions: Comparison of Literature Formulae and Artificial Neural Networks. *Journal of Hydroinformatics*, 13(4), 812–824. <https://doi.org/10.2166/hydro.2011.065>
- Tseng, M.-H., Yen, C.-L., & Song, C. C. S. (2000). Computation of Three-dimensional Flow around Square and Circular Piers. *International Journal for Numerical Methods in Fluids*, 34(3), 207–227. [https://doi.org/10.1002/1097-0363\(20001015\)34:3<207::AID-FLD31>3.0.CO;2-R](https://doi.org/10.1002/1097-0363(20001015)34:3<207::AID-FLD31>3.0.CO;2-R)
- Valela, C., Rennie, C. D., & Nistor, I. (2021). Improved Bridge Pier Collar for Reducing Scour. *International Journal of Sediment Research*, 37(1), 37–46. <https://doi.org/10.1016/j.ijsrc.2021.04.004>
- Wardhana, K., & Hadipriono, F. C. (2003). Analysis of Recent Bridge Failures in the United States. *Journal of Performance of Constructed Facilities*, 17(3), 144–150. [https://doi.org/10.1061/\(ASCE\)0887-3828\(2003\)17:3\(144\)](https://doi.org/10.1061/(ASCE)0887-3828(2003)17:3(144))
- Waskom, M. (2021). seaborn: Statistical Data Visualization. *Journal of Open Source Software*, 6(60), 3021. <https://doi.org/10.21105/joss.03021>
- Williams, P. (2019). *The role of Approach Flow and Blockage on Local Scour around Circular Cylinders with and without Countermeasures*. [Doctoral dissertation, University of Windsor]. Scholarship and UWindsor. <https://scholar.uwindsor.ca/etd/8154>
- Williams, P., Balachandar, R., and Bolisetti, T. (2013). Evaluation of Local Bridge Pier Scour Depth Estimation Methods. *Proceedings of the 24th Canadian Congress of Applied Mechanics held in Saskatoon*. Canadian Society for Civil Engineering (CSCE) Annual Conference, Saskatoon, Saskatchewan.
- Williams, P., Balachandar, R., Bolisetti, T., Roussinova, V., & Marrocco, M. (2019, June). Evaluation of Channel Blockage as a Governing Influence in Local Scour. *Proceedings of the 2019 Canadian Society of Civil Engineering Annual Conference in Laval*. Canadian Society for Civil Engineering (CSCE) Annual Conference, Laval, Quebec.
- Williams, P. D. (2016). *Scale Effects on Design Estimation of Scour Depths at Piers*. [MAsc thesis, University of Windsor]. Scholarship at UWindsor. <https://scholar.uwindsor.ca/etd/5117>
- Yanmaz, A. M., & Altinbilek, H. D. (1991). Study of Time-Dependent Local Scour around Bridge Piers. *Journal of Hydraulic Engineering*, 117(10), 1247–1268. [https://doi.org/10.1061/\(ASCE\)0733-9429\(1991\)117:10\(1247\)](https://doi.org/10.1061/(ASCE)0733-9429(1991)117:10(1247))

## APPENDICES

### **Appendix A: Software Acknowledgements**

The following open-source codes were used in this work:

- PyTorch (Paszke et al., 2019)
- Pytorch Lightning (Falcon et al., 2020)
- Optuna (Akiba et al., 2019)
- Seaborn (Waskom, 2021)
- Matplotlib (Hunter, 2007)

## Appendix B: Additional Results

### Field Model Results

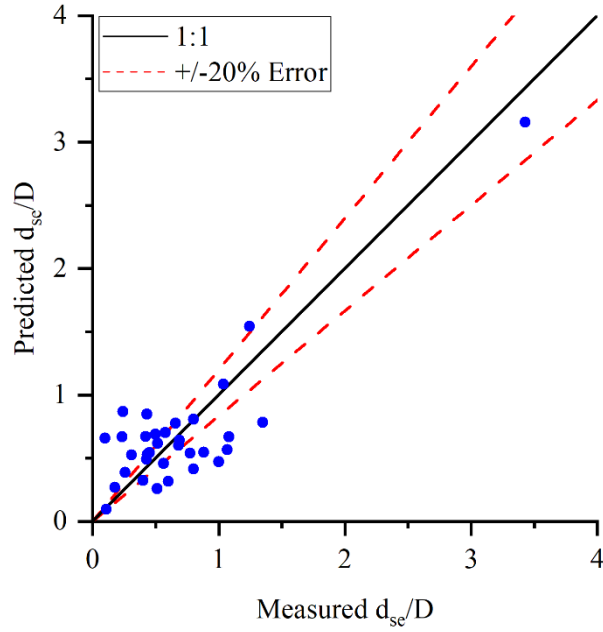


Figure B.1: Predicted vs. observed  $d_{sc}/D$  for field ANN with Neill shape factor

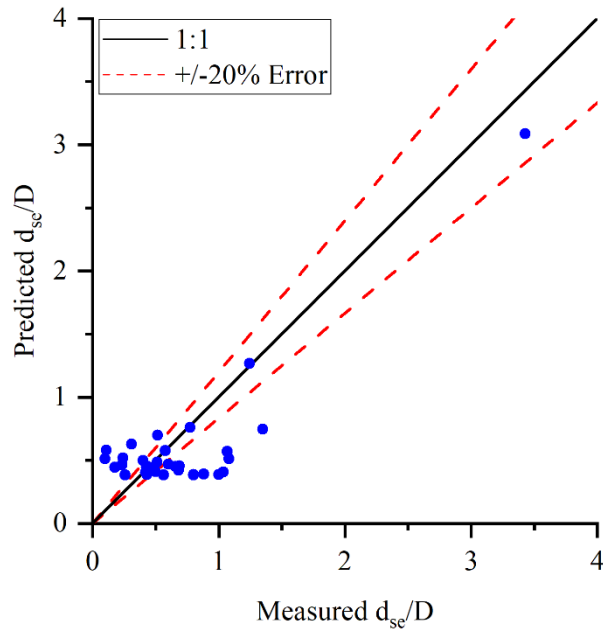


Figure B.2: Predicted vs. observed  $d_{sc}/D$  for field ANN with A&O shape factor

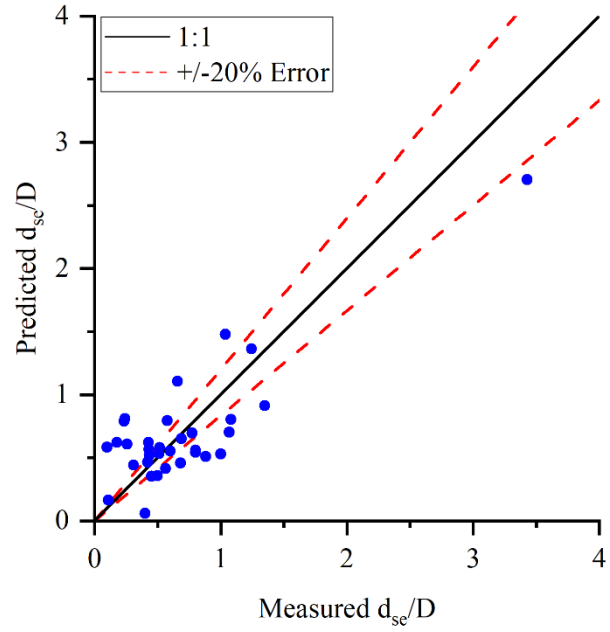


Figure B.3: Predicted vs. observed  $d_{sc}/D$  for field ANN with  $k$

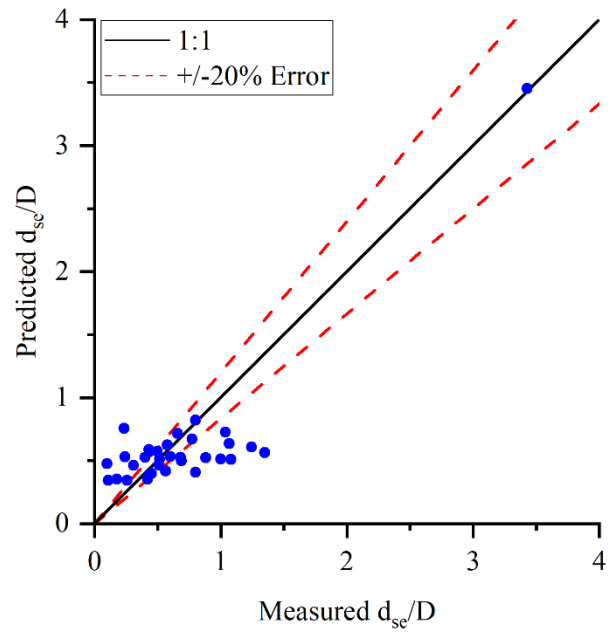


Figure B.4: Predicted vs. observed  $d_{sc}/D$  for field ANN with  $U_s/U_c$

## Combination Network

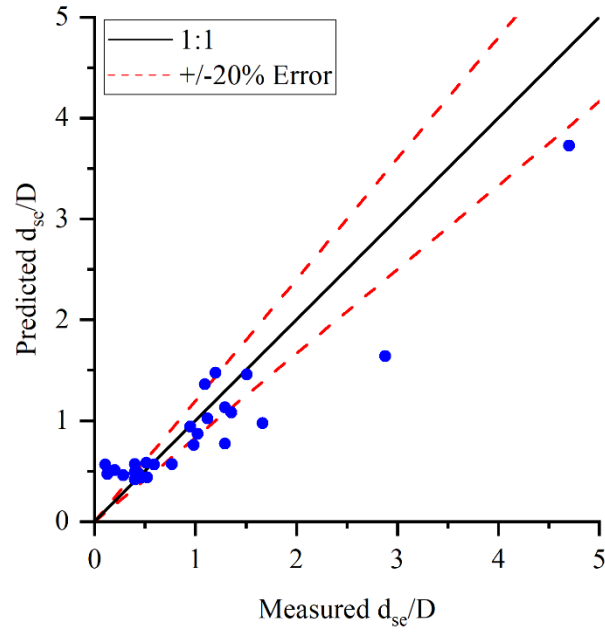


Figure B.5: Predicted vs. observed  $d_{sc}/D$  for combination ANN with HEC-18 shape factor

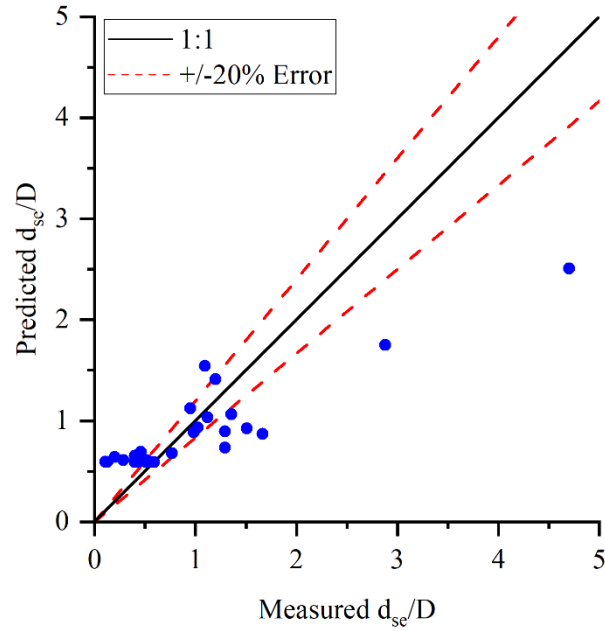


Figure B.6: Predicted vs. observed  $d_{sc}/D$  for combination ANN with Neill shape factor

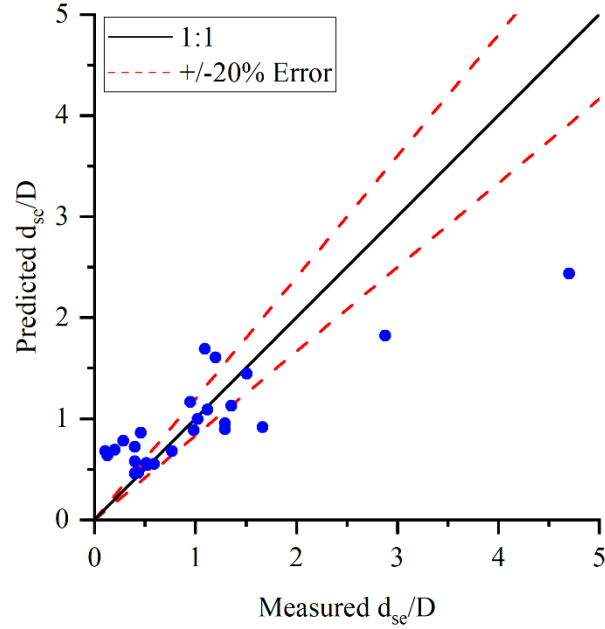


Figure B.7: Predicted vs. observed  $d_{sc}/D$  for combination ANN with A&O shape factor

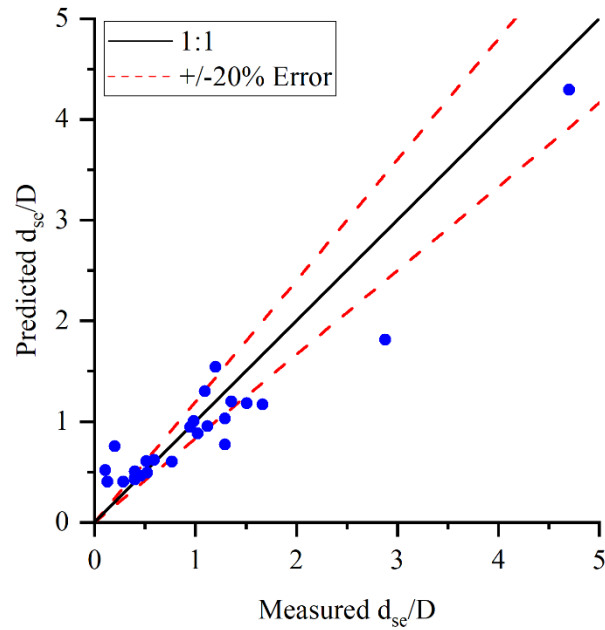


Figure B.8: Predicted vs. observed  $d_{sc}/D$  for combination ANN with  $k$

## Scour Width Network

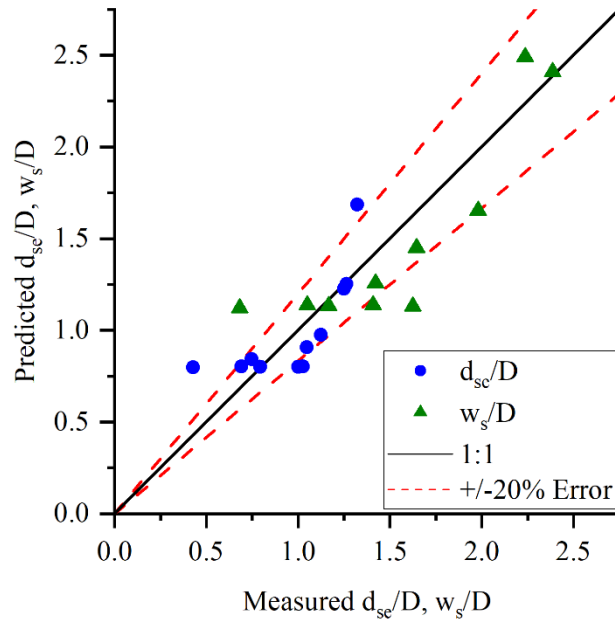


Figure B.9: Predicted vs. observed  $d_{sc}/D$  and  $w_s/D$  for scour width ANN re-optimized without  $D/B$

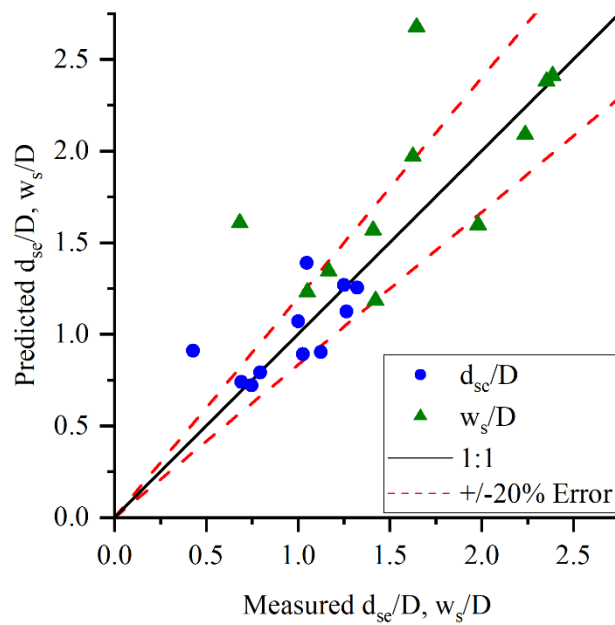


Figure B.10: Predicted vs. observed  $d_{sc}/D$  and  $w_s/D$  for scour width ANN with  $k$

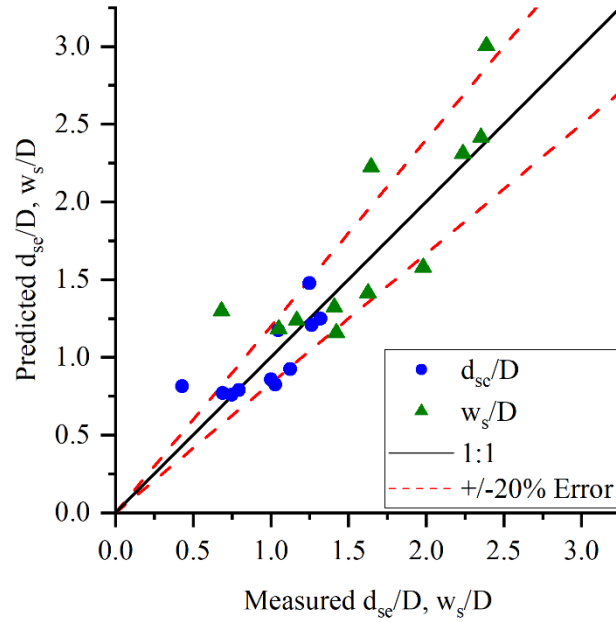


Figure B.11: Predicted vs. observed  $d_{sc}/D$  and  $w_s/D$  for scour width ANN with  $F_{ds}$

## VITA AUCTORIS

NAME: Mia Marrocco

PLACE OF BIRTH: Windsor, ON

YEAR OF BIRTH: 1998

EDUCATION: St. Thomas of Villanova  
Highschool, Windsor, ON, 2016

University of Windsor, B.A.Sc.,  
Windsor, ON, 2020

University of Windsor, M.A.Sc.,  
Windsor, ON, 2022